Answers to the reviewers

Previous title:
"Slope stability and rock fall hazard assessment of volcanic tuffs using RPAS with 2D FEM slope modelling".

Modified title:
"Slope stability and rock fall assessment of volcanic tuffs using RPAS with 2D FEM slope modelling".

Major changes in the manuscript:

- Text was rewritten and afterwards checked by a native speaker
- One new table (Table 1 – with image processing data) and 2 new Figures (Fig. 6 a DTM model, and Fig. 7. Differences between RPAS and TLS point clouds obtained by CloudCompare) were added according to the suggestions of the referee
- On Fig. 3 and on the new Fig. 7 the zone of potential rockfall is now marked (it was requested by the referee)
- Additional references were added describing the RPAS as a tool in obtaining images and the SfM - DSM generation and the use of such terrain models in slope stability assessment

Answer to the reviewer #1:

Thank you very much for your very constructive comments and suggestions. We have considered all of your comments and modified the manuscript accordingly. Please find **your comments in black** and our answers to your comments in red below.

REVIEW #1

The paper investigate the benefits to generate a DTM using a RPAS for engineering geology application. In particular, to use the DTM for slope stability analysis. In my opinion, the innovative contribute of this paper is quite limited in particular on RPAS point of view. DTM generation using RPSA is already a consolidated techniques, in particular nowadays is quite frequently used the use of oblique images for environmental application. This aspect could be an innovative contribute, but authors not have mentioned it.

In order to be considered for publication, it is mandatory to strongly modify several parts in the paper.

Comments:

Page 1: line9: "Low strength rhyolite tuff forms steep, hardly accessible cliffs in NE Hungary. The slope is affected by rock falls." What is the sense of these sentences? They are very generic. Moreover, the RPAS is not used to generate the DTM!!! RPAS is used to collect images, point clouds (with ALS), that can be used to generate a DTM or DSM (with vegetation). RPAS is only a tool!

That part of the abstract was corrected. We agree that RPAS is a tool and it collects images that need to be processed afterwards. The revised text takes into account this and has been modified according to the referee suggestions.

Page 1: line15: "The paper demonstrates that without RPAS…" This sentence is a little bit wrong, because it is possible to generate a digital model also with alternative method, as demonstrated in the last part of the paper.

We have reformulated the sentence, as RPAS based technology is capable to obtain reliable terrain information and useful input for geologic analyses.

Tachymetry is an old instrument, without EODM. Nowadays total station is used!! Please, replace tachymetry with total station at least!

We agree that tachymetry is a traditional measurement tool and nowadays total stations are used. Tachymetry was erased from the abstract, since the manuscript does not focus on it. The text was corrected accordingly and "total station" was used throughout in the main text of the manuscript.

Page 1 line 37-38…: this sentence is not clear.

The sentence was corrected.

Page 2, line 8-10: RPAS is not used to generate the hard surface, but it could help to acquire the images or point clouds. It is important to focus the attention about the planning and the data processing. To be improved.

The data processing of RPAS was described in detail in the revised text and a comparison with TLS was also provided. Uncovered rock surfaces were studied in this paper, where the RPAS captured images provide appropriate data for DSM. A new figure (Fig. 6) shows the DSM.

It is necessary to define the extension of the case study: how many hectares?

The study area is marked on Fig. 3, and now the zone where rock falls occur are also marked in the revised figs (red dot-and-dash lines).

Page 3: fig 2: it could be better to include the in the part a) the single index (b), c),..) close to the single box, c) is not clearly defined.

Fig. 2 was reshaped according to the comment.

Page4: fig3 : In the paper is many times mentioned the "risky zone for tourist", but it is not clearly where is this zone. Please, define this zone in the map. In this figure, north direction has to be included. Include a graphical scale.

On the revised Fig. 3, the zone that is affected by rock fall is marked (as well as on the new DTM on the new Fig. 6.). The direction of North is also marked on revised Fig. 3.

Caption fig3 is wrong: it is mentioned fig4, but fig.5 is the correct one. In figure 5 models are described and not the area. In the caption is said "the areas shown" but fig 5 has the model.

The Fig numbering was checked and it was corrected throughout the paper.

Page 4 line 5: it is not clear the "engineering geology" aspect. In fig 4 is not mentioned, but only geology. What is the difference between geology and Eng. Geology? To be clarified.

Engineering geology is a subtopic within the broader field of geology. It is a form of applied geology. We explain its role in slope stability assessment.

It is mentioned that flowchart are explained, but it is still very "poor" . to be better explained.

The flow chart is explained in more details.

Figure 4: some parts in the flowchart are not clear: connection between point cloud and cross section, or DEM and slope stability analysis.

Additional parts were added in the text explaining the flow chart and the flow chart was revised – the links between the parts of flow chart were also corrected.

Page 5 line4: it is not clear how the vegetation is removed. The authors declare that there are some part covered by vegetation. How the vegetation was considered? Alternatively, you have a DSM…Using TLS, it is possible to have directly a DTM.

Vegetation removal was done manually. At the studied area, mostly bare rock faces were found. However, some corrections were made. A new Fig (Fig. 6) shows the obtained DSM.

Page 5 from line 8: "The Remotely…" is not clear. Maybe the flight was done on 21st … It is important to describe better the flight planning, the % of overlapping, etc. In other words, it is necessary to include a table with all information about the flight. One question: how is possible to guarantee the correct overlapping with a manual flight, with a limited vision of the UAV? What is the GSD? What is the relative height? How the camera calibration has been realized? Go pro is a very hard camera to be calibrated.

We have already indicated in the text that there was no prior flight planning. The weather was not exactly fine for the RPAS-flight, because it was somewhat windy. The skilled pilot could control the drone with the help of the FPV option, so the required image overlap could be ensured. The weather conditions explain the variety of the flying height (60-100 m relative flying height). The average GSD was therefore 3-5 cm on the ground. The applied software (Pix4D) has also a camera calibration option, thus no prior camera calibration was planned and executed. We agree with the reviewer that the calibration of GoPro camera is hard, but TLS was used for the validation. A comparative analysis of point clouds of RPAS and TLS is given on the new Fig. 7. On the other new figure, on Fig. 6, the ground control points that were used for referencing are also shown.

Remarks: why have you not considered to collect oblique images?
http://www.itc.nl/library/papers_2016/pres/nex_obl_ppt.pdf

Thank you for the comments and suggestion as well as for the suggested references on oblique images. We used that in the paper and cited some of those references. The field data was collected by using RPAS and the data was validated and cross checked by TLS. We believe that the obtained data quality proved that with the use of manual controlled RPAS it is also possible to obtain high quality data.

The number of points in the cloud is drastically limited with respect TLS, why? You have 3 flight…In my opinion 12 million of points is very poor for your area.

We fully agree that TLS has much more captured points than required. One reason is that the region of interest is smaller than the scanned area. The next reason is that the geological analyses do not require such a high resolution data set, thus we have decided to resample the data set. The amount of the RPAS points was mentioned wrong; since nearly 19 million points were derived by the photogrammetric data evaluation. The typo has been corrected in the text.

Page 6 line 7: where do you have placed the GCP? Include a map.

GCPs are illustrated in the newly inserted Figure 6 (DSM).

Page 6 line 13: typos.

Typos have been corrected.

Page 6 line 14: a point cloud comparison is mentioned by cloud compare, but it is not shown and described. Figure 4 mentioned is related to another part. TO BE INTEGRATED. IT IS VERY IMPORTANT TO COMPARE TLS SOLUTION WITH SFM SOLUTION.

CloudCompare is a well-known and widely used software tool to compare point clouds and the derived models. The original text has been extended by new text and new citations as well as a new comparative Figure (new Fig. 7) has been inserted showing the differences between RPAS and TLS point clouds. It marks clearly that the analyzed point clouds are very similar; as the highest difference is less than 0.1 m. Figure citation was corrected.

Pag7: line 2: Figure 7. In figure 7 is not shown the model. To be correct or include a new figure

It was corrected in the text.

Pag7: line 3: Figure57. In figure5 is not shown the CAD model, as mentioned here.

Referencing to Fig. 7. has been removed.

Page 7 line 8: you mention some details in figure 4, but they are not described. (as morphological index). It is necessary to define and to describe how you calculate these indexes. Equations are required

The DSM/DEM based analyses are built-in functions in GIS software SAGA. Some of these features are documented. The morphological index functionality is further referenced with the revised paper. Unfortunately these indices can not be described by using an equation, because most of them are coming from a sophisticated algorithm. These are usually too complex for a single equation, but the method was referenced in the text.

Page 7 line 12: where do you mention the engineering geology? Not clear.

Engineering geology is an applied geology that also deals with slope stability. It is a widely used expression, and an Engineering Geology journal also exists.

Page 7 line 29: you have to define this area in the figure 3!

The zones where rock falls occur are marked in the revised Fig. 3 and also on the new fig showing DTM (Fig. 6).

Page 7 line 35: …"from RPAS (DTM model figure 4)". In figure 4 is not shown a DTM…to be clarified.

It was explained more clearly in the revised manuscript and a new figure was also inserted in the text that shows DSM (Fig. 6).

Page7 line 2: " DTM and morphological…"where? It is not defined in the paper.

We guess that the reviewer refers to Page 9. The text was corrected and rewritten.

Caption figure 7: "…from DEM analysis (fig 4)…where?? How?...not defined in the paper.. RPAS dataset has not sense!

The figure caption of Fig. 7 (in the revised paper this figure is Fig. 9) was corrected.

Page 10 line 5: figure 4 is mentioned but it is a mistake.

The mistake was corrected. The correct reference is: Fig. 3.

Page 10 line 14-15: sentence very poor. To be clarified. It is not clear the DTM analysis.

That part of the paper was rewritten.

Page 11: it is not clear what is the site where the analysis is carried out.

The kinematic analyses were made for rock joints: planar and wedge failure was calculated. 6 major sets of rock joints were identified (see text and Fig. 11 and Fig. 12.). These joints are located in the area, which are marked on Fig. 3 as a zone that is affected by rock fall.

DISCUSSION SECTION has to be deeply reviewed.

Page 12 line 7-11: no comparison between TLS and SFM solution is made. It is not possible to verify the conclusion here reported.

A new figure is inserted in the text which provides information on the point clouds of RPAS and TLS (new Fig. 7). It is better explained now in the revised text, too.

Page 12 line 15-18: to be defined better this declaration.

Fig. 7 proves that the differences between RPAS based and TLS based terrain models are minor, and thus RPAS is an excellent tool to solve slope stability problems.

Page 12 line 19-26: to be defined how to realize that. SFM is a technique quite influenced by the shadow, in contrary to TLS system. Not very clear what you want to demonstrate. It is not very ease to reconstruct a correct DTM with SFM, if the data acquisition is not correctly made.

The flight was executed in leaf-free season; otherwise the most interesting areas were not covered by vegetation. If some vegetation was captured, they were filtered out from the results. The minor effect of vegetation is clearly seen on Fig. 6, but fortunately the zones that were interesting for slope stability analyses were bare cliffs and were not covered by vegetation.

Page 13: this part is very critical. You have to better motivate how you built this table and why you have defined this index, with a literature support! The content is partially in opposite with the table 3. To be completely reviewed.

The table was omitted and the differences were explained in more detail in the Discussion part of the revised text.

Page 13 line 21: typos tachmietry

Thank you for your remark, the typo has been corrected.

Conclusion. This part needs a very hard review. IT could be interesting to have a comparison between the analysis made using SFM solution and using TLS dataset, just to compare the difference, accuracy and more.

The conclusions were rewritten.

The use of RPAS for photogrammetry is a consolidated technique, even in geology than ir order to be published, it is necessary to give a more innovative definition.

New data sets are added in the paper with new figures and corrected figures. The text was also rewritten at parts focusing on the applicability of RPAS in cliff stability analysis and the appropriate resolution of RPAS validated by TLS.

Review #2:

Answer to the reviewer #2:

We really appreciate the comments and suggested corrections. We have considered your suggestions and modified the manuscript accordingly. Please find **your comments in black** and our answers to your comments in red below.

Dear Editor, dear Authors:

General comment: The manuscript has improved from the first version, but still has lingering issues that need to be addressed and does not contains enough details to make the analysis fully understandable.

Specific comments:

1)Several issues with sentence structure and grammar still persist. I would recommend a further English edit to improve sentence structure and terminology.

The terminology was updated and a native speaker corrected the English text.

2)The authors use (in the title and at some points in the text, e.g. page 3, line 9) the term hazard assessment to describe their analyses. Since the rock fall hazard assessment requires specific data (e.g. frequency and magnitude) and further analyses (e.g. trajectory modeling) that are not presented in the text, I would suggest remove it from the title and the text. Please be specific and use the appropriate terms in the description of the analysis.

This term 'hazard' has been removed from the title and also from the text.

3)It is not clear from the text how the model obtained with RPAS based photogrammetry was validated using TLS data and which is its accuracy. Please explain the method adding specific details.

The RPAS based photogrammetry was validated by using TLS. A detailed explanation is given in the revised text and a new figure (Fig. 7) was added showing the differences between the point clouds obtained by RPAS and TLS.

4) The authors state that "the rock mass failure was analyzed with the RocFall FEM software of the Rocscience (RS2)". For what I know the RocFall software is a trajectory simulation software and does not allow to analyze the stability of a slope. Please verify and in case modify the text.

In the revised paper we have explained more how the RocScience software was used and SRF factor is explained with a modified Fig (now Fig. 9, in the previous manuscript it was Fig. 8). No trajectories were modelled.

5)It is not clear from the text how discontinuity measurements were extracted from the RPAS based photogrammetric model. This is a key aspect to underline the potential of using the RPAS based photogrammetry in rock slope stability analysis and kinematic analysis of discontinuity sets. Please clarify.

The set of discontinuities are now described better, and on Fig. 11 and Fig. 12, the main joint sets are marked. A new figure Fig. 6 shows the DSM model and the text explains how the orientation of discontinuities was obtained by using the catchment area diagram (Fig. 9). It was also validated by field measurements and 6 main joint sets were identified (see text and Fig. 11 and Fig. 12).

6) At line 7 of page 8 (and in the flow chart of figure 4) the authors state that "Risk assessment was based on slope stability calculation" but no risk analysis is presented. Please modify the text considering the real

contribution of the analysis.

The risk assessment was not performed but slope stability analyses were made. Accordingly, in agreement with the referee's comment, Fig. 4 was modified and the term 'risk assessment' was not used in the text.

7) The authors state that "six main joint sets (…) were identified with prevailing NE-SW direction" and refer the text to figure 7. From the text, it is not clear what criterion is used to show joint measurements (e.g. dip/strike or dip/dip direction); it seems that measurements in the text are indicated as dip/dip direction and in the rose diagram of figure 7 as dip/strike (it is not obvious for the reader). Moreover, for what I can understand looking at figure 7, it shows only 5 joint sets and two of that have a very similar strike (I suppose strike 312 and 299). Please clarify this aspect adding specific details in the text and in the caption of figure 7.

The text was rewritten. The rose diagram shows the orientation of major discontinuities (see Fig. 9). The set of discontinuities are now described better and on Fig. 11 and Fig. 12 (previously Fig. 9 and Fig. 10); the 6 main joint sets are marked. The orientation of the 6 main joint sets is also listed in the text and it was added that dip angle/dip directions are given.

8) In the cross sections of figure 8, the authors indicate the total displacement (see caption) with color ranging from blue to red and do not show any color scale to relate displacement values to colors. In this way, it is not clear what the reader should conclude looking at the analysis, also considering that despite the safety factor is above 1 the slope is subject to deformation. Please clarify this aspect and show the result of the stability analysis for all of the selected cross sections.

The total displacements are now given on the new Fig. 10 (previously Fig. 8) and the text was reshaped accordingly.

9)In the conclusions the authors state that "According to 2D FEM modeling the intercalating low strength layer is one where potential slip surface can develop causing larger scale mass movements, but at present it has low probability". Even if this interpretation might be consistent with a modeled spatial distribution of the safety factor (that is not shown in the specific figure), in my opinion the result of the global stability analysis is not suitable to estimate the probability of occurrence of a landslide. Please modify the sentence or remove.

The sentence was corrected and the conclusions were rewritten.

With the above corrections, I feel the manuscript may be reconsidered for publication.

Slope stability and rock fall ~~hazard~~ assessment of volcanic tuffs using RPAS with 2D FEM slope modelling

Ákos Török[1], Árpád Barsi[2], Gyula Bögöly[1], Tamás Lovas[2], Árpád Somogyi[2], and Péter Görög[1]

[1]Department of Engineering Geology and Geotechnics, Budapest University of Technology and Economics, Budapest, H-1111, Hungary
[2]Department of Photogrammetry and Geoinformatics, Budapest University of Technology and Economics, Budapest, H-1111, Hungary

Correspondence to: Ákos Török (torokakos@mail.bme.hu)

Abstract. ~~Low strength rhyolite tuff forms steep~~Steep, hardly accessible cliffs of rhyolite tuff in NE Hungary~~. The slope is affected by~~ are prone to rock falls~~.~~ endangering visitors of a castle. Remote sensing techniques were employed to obtain data on terrain morphology and to provide slope geometry for assessing the stability of these rock walls. RPAS (Remotely Piloted Aircraft System) was used to collect images which were processed by Pix4D mapper (Structure-from-Motion technology) to generate a point cloud and mesh. The georeferencing was made by Global Navigation Satellite System (GNSS) with the use of 7 ground control points. The obtained digital ~~terrain~~surface model (DSM) was processed (vegetation removal) and the derived Digital Terrain Model (DTM) ~~for slope stability analysis and rock fall hazard assessment. Cross~~allowed to draw cross sections and to detect joint system ~~data was obtained from DTM.~~ Joint and discontinuity system was also verified by field measurements. On site ~~and~~as well as laboratory tests provided additional engineering geological data for slope modelling. Stability of cliffs ~~and rock fall hazard were~~was assessed by 2D FEM (Finite Element Method). Global analyses of cross-sections show that weak intercalating tuff layers may serve as potential slip surfaces, however, at present; the highest hazard is related to planar failure along ENE-WSW joints and to wedge failure. The paper demonstrates that ~~without~~ RPAS ~~no~~is a rapid and useful tool of generating reliable terrain model ~~could be made and it~~of hardly accessible cliff faces. It also emphasizes the efficiency of RPAS in rock fall hazard assessment in comparison with other remote sensing techniques such as terrestrial laser scanning (TLS~~) and tachymetry.~~).

1 Introduction

In the past years, technological development of RPAS revolutionized the data gathering of landslide affected areas (Rau et al. 2011), recultivated mines (Haas et al. 2016~~),~~) and the monitoring of coastal processes (Casella et al. 2016), and levee breaches (Brauneck et al. 2016) or road cuts (Mateos et al. 2016). ~~-~~RPAS has been increasingly used in engineering geology~~;~~ in historical landslide mapping (Jovančević et al. 2016) and in slope stability analyses (Niethammer et al. 2012, Fraštia et al 2014) as well as in other natural disasters such as earthquakes (Gerke & Kerle 2011, Nex et al. 2014) or floods (Feng et al. 2015). ~~,) RPAS can~~RPAS can also be combined with terrestrial laser scanning (TLS) since both remote sensing tools provide high precision terrain measurement (Fanti et al. 2013, Assali et al. 2014, Francioni et al. 2014, ~~Neugrig~~Neugirg et al. 2016, Manconi & Giordan 2015). These tools can be used to validate height information derived by other technologies. Rock falls represent special landslide hazards since their rapid movements and various trajectories make it difficult to predict their hazard potential (Crosta & Agliardi 2003, Manconi & Giordan 2014). Several methods have been suggested to assess cliff stability ranging from physical prediction rock fall hazard index (Crosta & Agliardi 2003) via Rockfall Hazard Rating System (Budetta 2004) ~~and~~to the modelling of their trajectories (Crosta & Agliardi 2002, Abbruzzese et al. 2009, Copons et al. 2009, Samodra et al. 2016). These methods rely on understanding failure mechanisms and on predicting displacement of rock masses (Pappalardo et al. 2014, Stead & Wolter 2015, Mateos et al. 2016~~)~~), or ~~at~~in some cases, on predicting displacement of individual rock blocks (Martino & Mazzanti 2014). To gather data on the rock fall hazard of existing cliff

faces, a number of crucial data is needed: slope profiles, material properties, block size (De Biagi et al. 2017~~)~~), and possible discontinuity surfaces that can contribute to slope instability. Slope profiles can be obtained from point clouds, while material properties have to be measured on site (e.g. Uniaxial Compressive ~~Strenght~~Strength by Schmidt hammer) or under laboratory conditions (Margottini et al. 2015). ~~Detection~~For the detection and mapping of joints ~~require fieldwork (on site measuring by compass), or at hardly accessible locations~~and fractures it is possible ~~by applying~~to apply remote sensing techniques (Fanti et al. 2013~~), or both.~~, Tannant 2015, Salvini et al. 2017).

Most ~~of~~ rock fall hazard publications deal with hard, well cemented rocks, such as limestone (Samodra et al. 2016~~)~~), or various other types of sedimentary rocks (Michoud et al. 2012~~),~~) such as igneous or metamorphic rocks. In contrast, very few previous studies deal with cliff face stability and rock fall hazard of low strength rock such as volcanic tuffs (Fanti et al. 2013, Margottini et al. 2015). Volcanic tuffs are very porous rocks and are prone to weathering (Arikan et al. 2007). While the current paper deals with a low strength pyroclastic rock, it has a slightly different approach of cliff stability analysis~~,~~ ~~since~~. In this study, slope stability is assessed by using a combination of remote sensing techniques, field measurements, and laboratory testing of tuffs with 2D FEM (Finite Element Analysis) analyses of slopes. ~~Compared~~In contrast to other case studies, this study operates on a smaller scale and studies the possibilities of wedge and planar failures. ~~The~~More specifically, in our context, the cliff face is unstable as it is evidenced by falling blocks. Due to rock fall hazard, the small touristic pathway was closed to avoid causalities. The current paper analyses the cliff faces by condition assessment and stability calculations. Thus, this research provides an assessment of how RPAS-based images and photogrammetric processing can be used to ~~create~~derive a surface model at ~~hardly accessible~~ sites that are difficult to access. The paper also demonstrates the combined use of photogrammetric, surveying, and engineering geological methods at difficult ground conditions in assessing rock slope stability.

2 Study area

The study area is located at mid~~–~~mountain range in NE-Hungary~~. A~~, where a hardly accessible jointed rhyolite tuff cliff face was studied. On the top of the cliff, a touristic point, the Sirok Castle is located (Fig. 1~~). The~~), with the steep rhyolite tuff hill with an elevation of 298 m ~~and found~~ at the transition area of two mountain ranges, Mátra and Bükk Mountains. The tuff is very porous and prone to weathering (Vásárhelyi 2002, Kleb &Vásárhelyi 2003, Török et al. 2007).

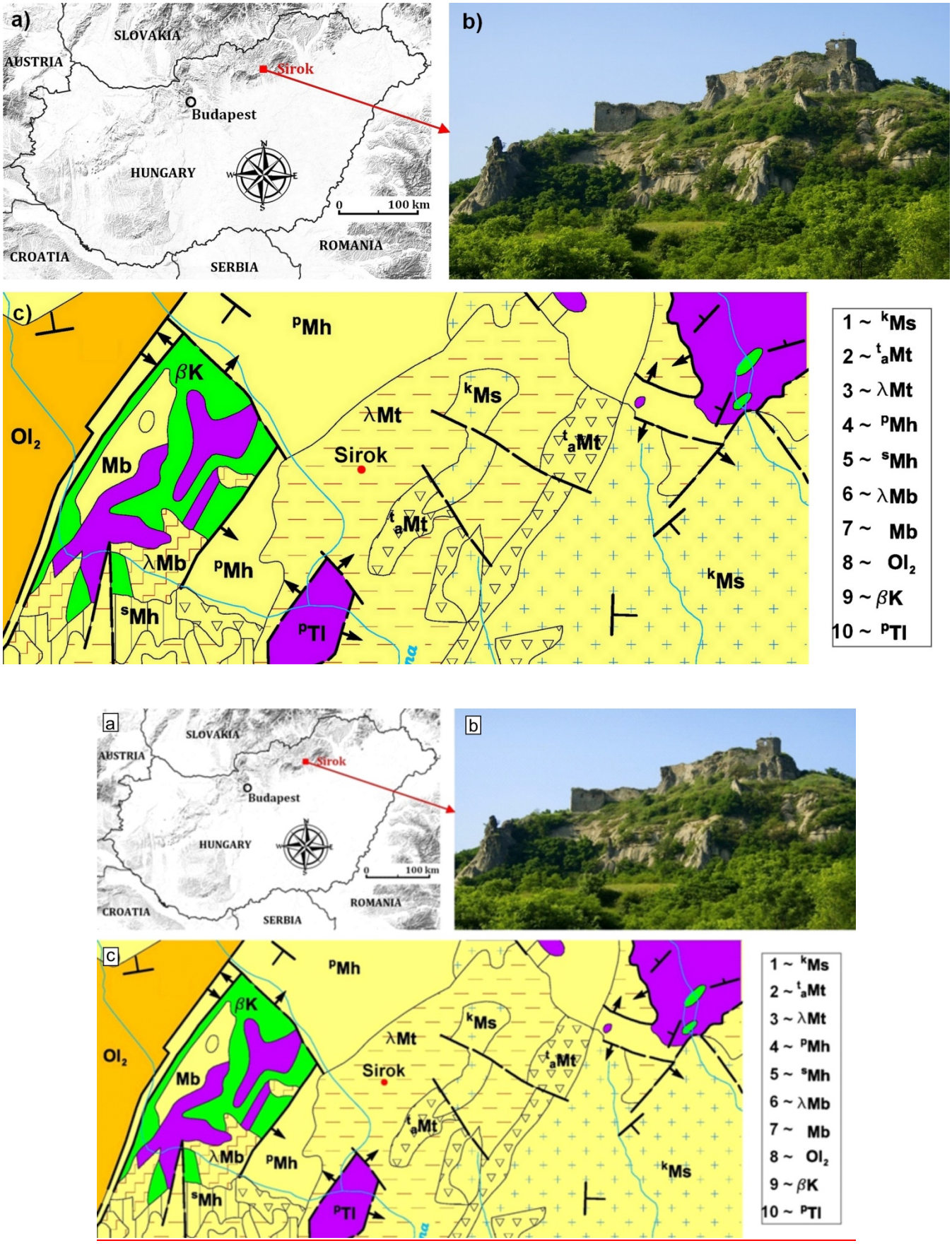

a
SLOVAKIA
AUSTRIA
Sirok
Budapest
HUNGARY
0 100 km
ROMANIA
CROATIA
SERBIA
b
c
^{P}Mh
βK
Ol$_2$
Mb
λMt
^{k}Ms
Sirok
$^{t}_{a}$Mt
λMb
^{P}Mh
^{s}Mh
^{P}Tl
^{k}Ms
1 ~ ^{k}Ms
2 ~ $^{t}_{a}$Mt
3 ~ λMt
4 ~ ^{P}Mh
5 ~ ^{s}Mh
6 ~ λMb
7 ~ Mb
8 ~ Ol$_2$
9 ~ βK
10 ~ ^{P}Tl

Fig.1. Location of studied cliff faces and an image of the rocky slope at Sirok Castle, NE Hungary (top) and the geological map of the area (redrawn after Balogh 1964) (bottom). Legend for geological map: Miocene (1-7), Oligocene (8), Cretaceous (9), Triassic (10): 1: gravel and conglomerate; 2: clay; 3:rhyolite tuff; 4: sand and sandstone; 5: siltstone; 6: rhyodacite tuff; 7: fine sand; 8: clay; 9: basalt; 10: radiolarite.

Although the first castle was already constructed in the 13th century AD, due to war damages and reconstructions, the current structure encompasses wall sections representing different construction periods. In these days, the partially ruined walls have been restored, and the castle is open to tourists, but southern slopes are closed due to rock fall hazard.

The hill represents a rhyolite tuff that was formed during the Miocene volcanism (Badenian-Lower Pannonian period). The cliff face was formed during to the late Miocene volcanic activity. It, and is a part of the Inner Carpathian volcanic chain. The geological map of the closer area clearly reflects the dominance of pyroclastic rocks, with isolated occurrences of Oligocene and Triassic rocks (Fig. 1). The cliffs are steep and display several joints and discontinuity surfaces. The present study focuses on the southern hillslope of the castle hill, where major rock falls occurred in the near past (Fig. 2). The study area is divided into smaller units, where RPAS and rock fall hazard assessment analyses were carried out (Fig 3).

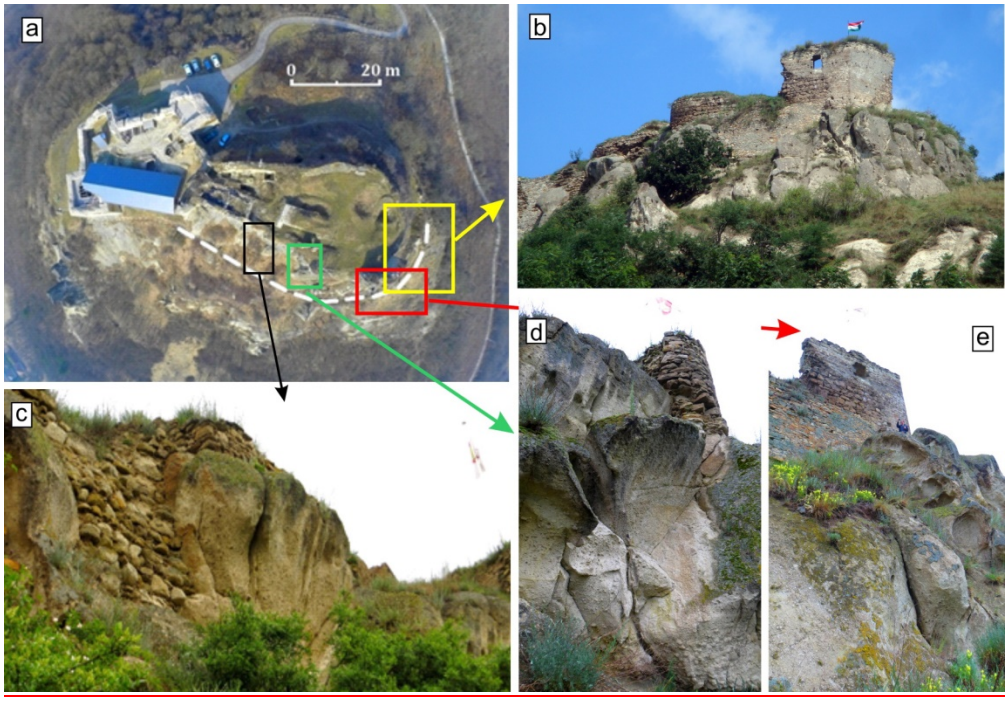

Fig.2. Studied southern cliff faces ~~(clockwise):~~: a) image of the castle obtained by RPAS with marked details; b) distant view of the eastern part of the cliff section; c) ~~weathered rounded cliff with larger taffoni~~steep cliffs dissected by joints; d) vertical to sub-vertical cliff face with steep joints and traces of rock fall~~;~~ and e) ~~steep cliffs dissected by joints~~weathered rounded cliff with larger taffoni.

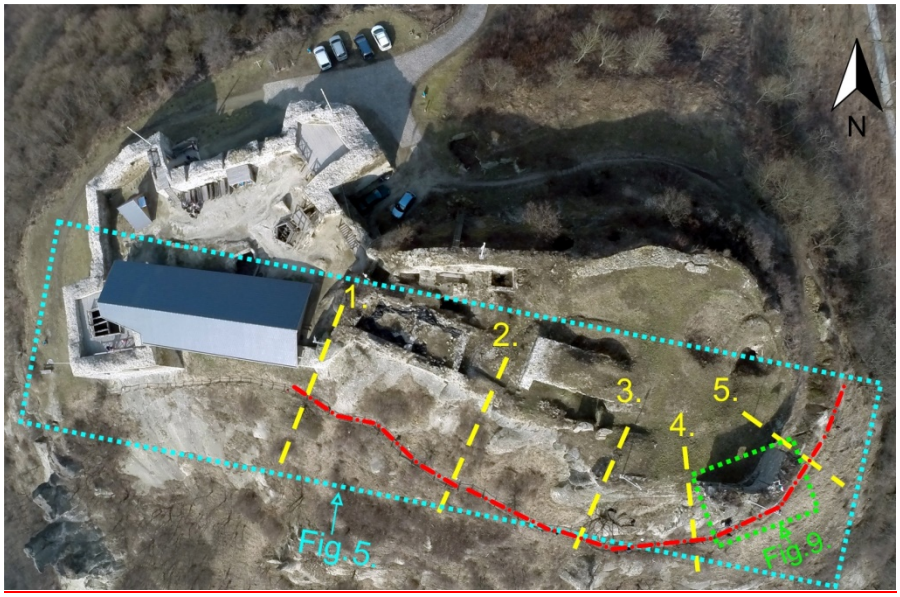

Fig.3. Location of the illustrations in the paper and the ~~sections (1 to5 marked~~rock fall affected area. Red dot-and-dash line represents zones affected by ~~yellow~~rock fall. Yellow dashed lines~~)~~ 1 to 5 mark the sections where slope stability was calculated by using 2D FEM model (Fig.8). Dotted lines indicate the areas shown on Fig. ~~4~~5 and Fig. ~~7~~9.

3 Materials and Methods

The research contains two major methods: i) RPAS and ii) engineering geology. The applied methods are summarized in a flow diagram displaying the combination and links between the two methods (Fig. 4). The flow chart has four major realms that have both RPAS and engineering geological units: i) preparation; ii) field survey; iii) data processing and calculation and finally interpretation. The RPAS line is described in details in the next part of the paper, but also linked to previous publications providing overview of image acquisition, image processing and interpretation (Civera et al. 2012, Westoby et al. 2012, Remondino et al. 2014).~~(Fig. 4). The explanation of these research methods are given below in more details.~~ Engineering geological part of the flow chart is also explained below, but also has strong links to publications describing the application of RPAS to landslide characterization, and rock slope stability assessment (Niethammer et al. 2012, Tannant 2015).

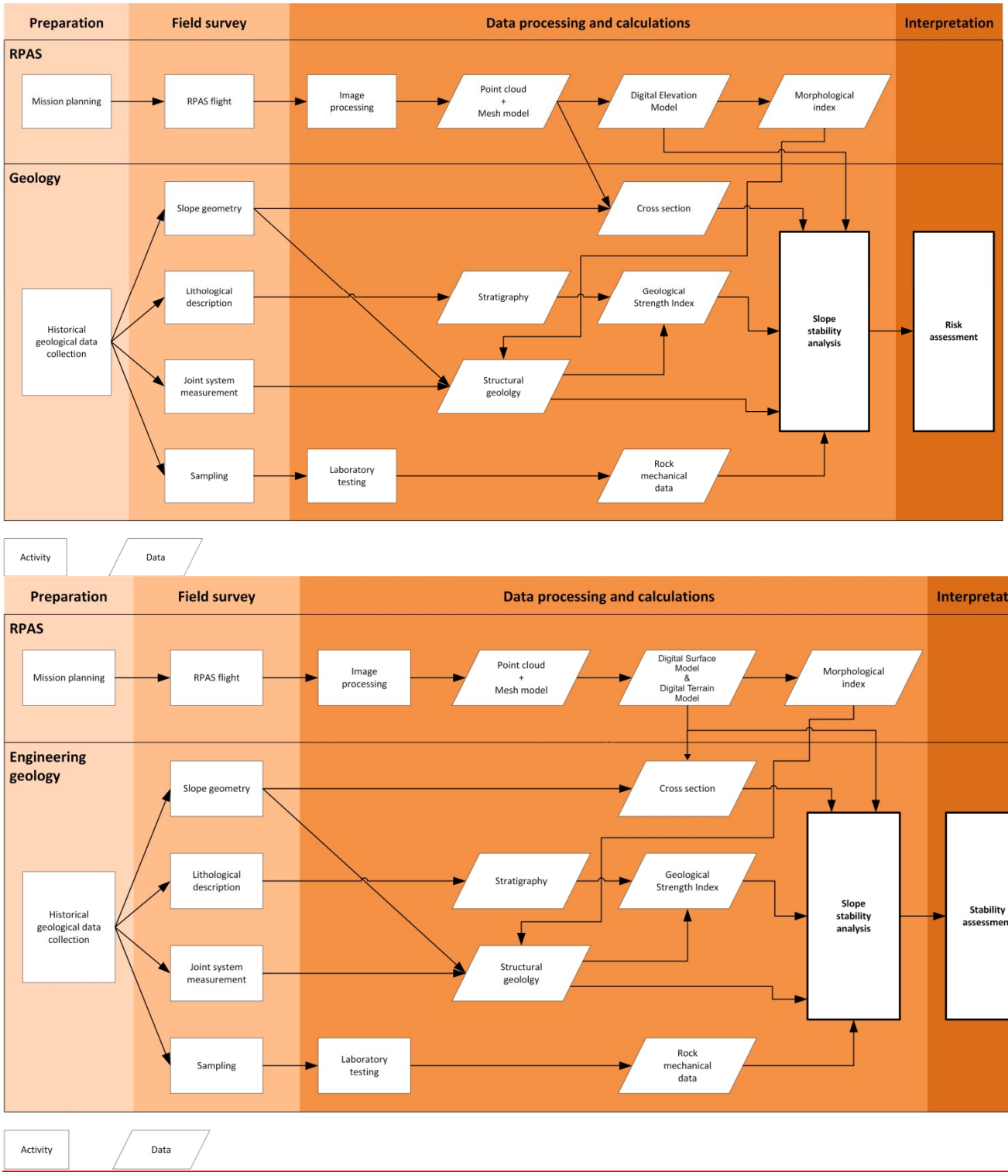

Fig.4. Flow chart showing the methods and obtained data set of this paper indicating the interrelationship between RPAS, ~~geological analyses and risk~~slope stability assessment (see details in the text)

3.1 RPAS data acquisition and terrain modelling

~~For cliff stability analysis a digital terrain model was required. It assumes the accurate 3D modelling of the highly dissected rock faces. Since major parts of the site consist of hardly accessible steep slopes that are partly covered by vegetation, traditional surveying was not possible. As a consequence, RPAS technology was applied (Fig. 4).~~ ~~By the use of RPAS, high~~

~~amount of images was captured, and then a 3D point cloud was generated to enable surface modelling. The point cloud was validated by terrestrial laser scanning, which is a mature, widely used technology in creating detailed, accurate surface models.~~

The Remotely Piloted Aerial System (RPAS) was deployed on 21st February 2015, when vegetation cover was limited. The remaining vegetation was manually removed; luckily, the areas with the highest hazard were barely covered. The system is a modified commercial DJI Phantom 2 drone (DJI, ~~2016~~2015), where the flying vehicle has been equipped with a synchronous image transfer (First-Person Viewer – FPV) option that also forwards the current flying parameters (e.g. height, speed, tilt, power reserve). Due to the complexity of the survey area, the flight was controlled manually; the required overlap between images was ensured by the operator considering capture frequency. The necessary overlap between images was controlled by the FPV option. For safety reasons, the crew consisted of two persons: one for controlling the aircraft, and the other one for continuously monitoring the transferred video stream. The camera control ~~is~~was done by a tablet.

A GoPro Hero 3+ (GoPro, 2017) action camera was mounted onto a 2-DoF gimbal of the unmanned aerial vehicle (UAV). The camera has a fixed 2.77 mm focal length objective that is capable of capturing 4000 × 3000 pixel sized JPG images. The images were captured with a sensitivity of ISO 100 and ~~sRGB color~~RGB colour space. The lens was used with a fixed aperture of 2.8 and the camera was able to adjust the adequate shutter speed. Generally, the exposure time was set to 1/1400 s and the images were compressed at a rate of 4.5 bits/pixel. There were three imaging flights; two around noon and one at about 5 in the afternoon. The flying times were 13, 12 and 13 minutes, respectively, where 390, 365 and 419 images were captured. All 1174 images were involved in the photogrammetric object reconstruction (Fig. 5). The photogrammetric reconstruction has been done by Pix4Dmapper (Pix4D, 2017), which is based on Structure-from-Motion (SfM) technology (Lowe 2004, Westoby et al. 2012, Danzi et al. 2013~~, Lowe 2004).~~,). SfM automatically identifies tie points considering initial requirements (e.g. preliminary image centre positions, time stamps) (Table 1). Camera calibration was executed during post-processing, and no prior calibration was needed~~.~~ (Pix4D, 2017). After the image alignment, the image projection centres and attitudes can be observed ~~in~~ (Fig. ~~4). 12~~5). 19.3 million points were obtained by the photogrammetric reconstruction, which was appropriate for the engineering geological application, however the technology allows to obtain higher resolution, but it was not necessary. The average point density is about 670 points/m^3, but there are areas, where double point density.

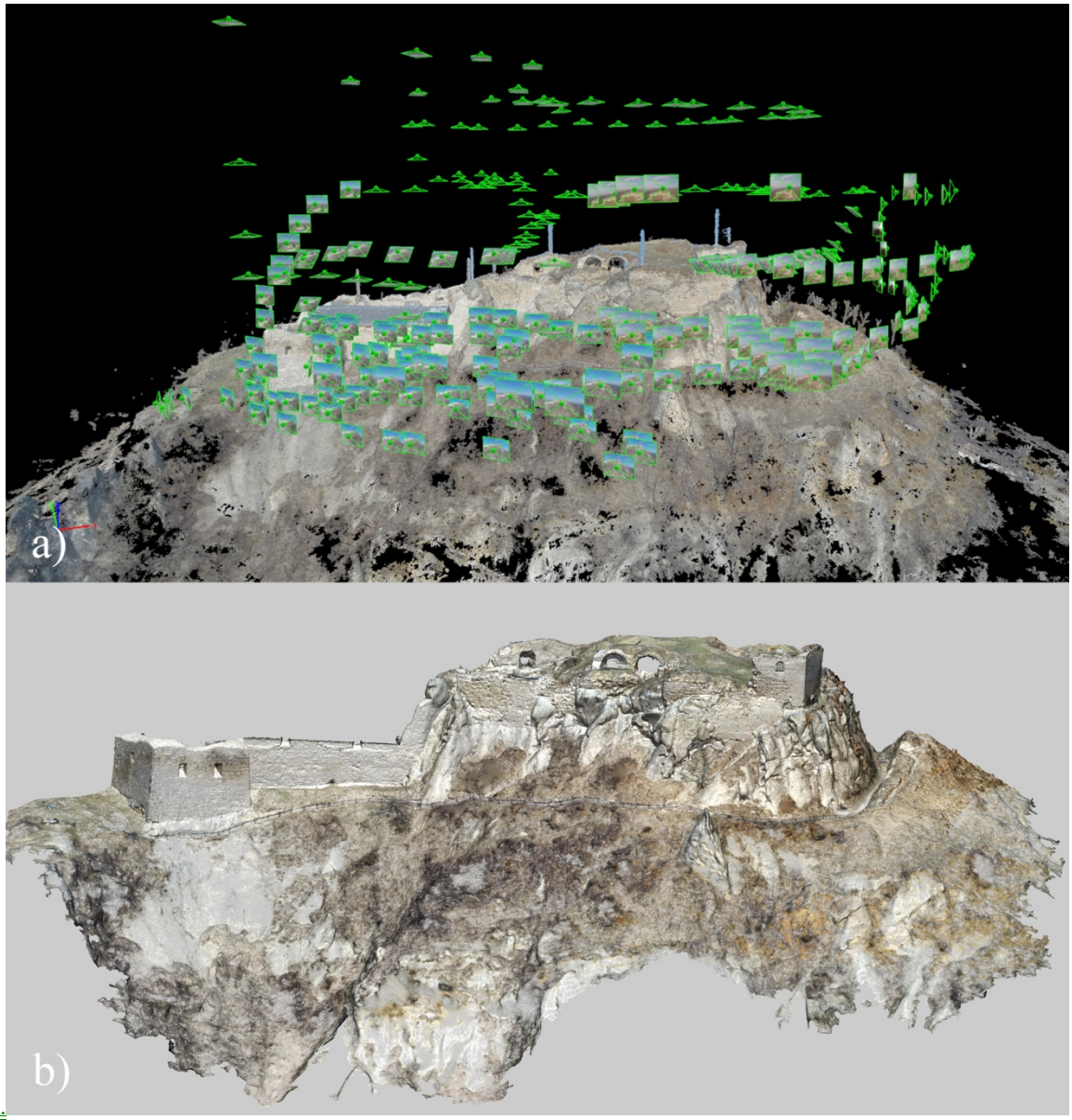

Table 1.

Image processing data

Mean number of keypoints per image	22676
Mean number of matched keypoints per image	9546
Mean reprojection error [pixel]	0.176
Time for SfM processing	40m:20s
Time for densification (point cloud)	05h:30m:24s

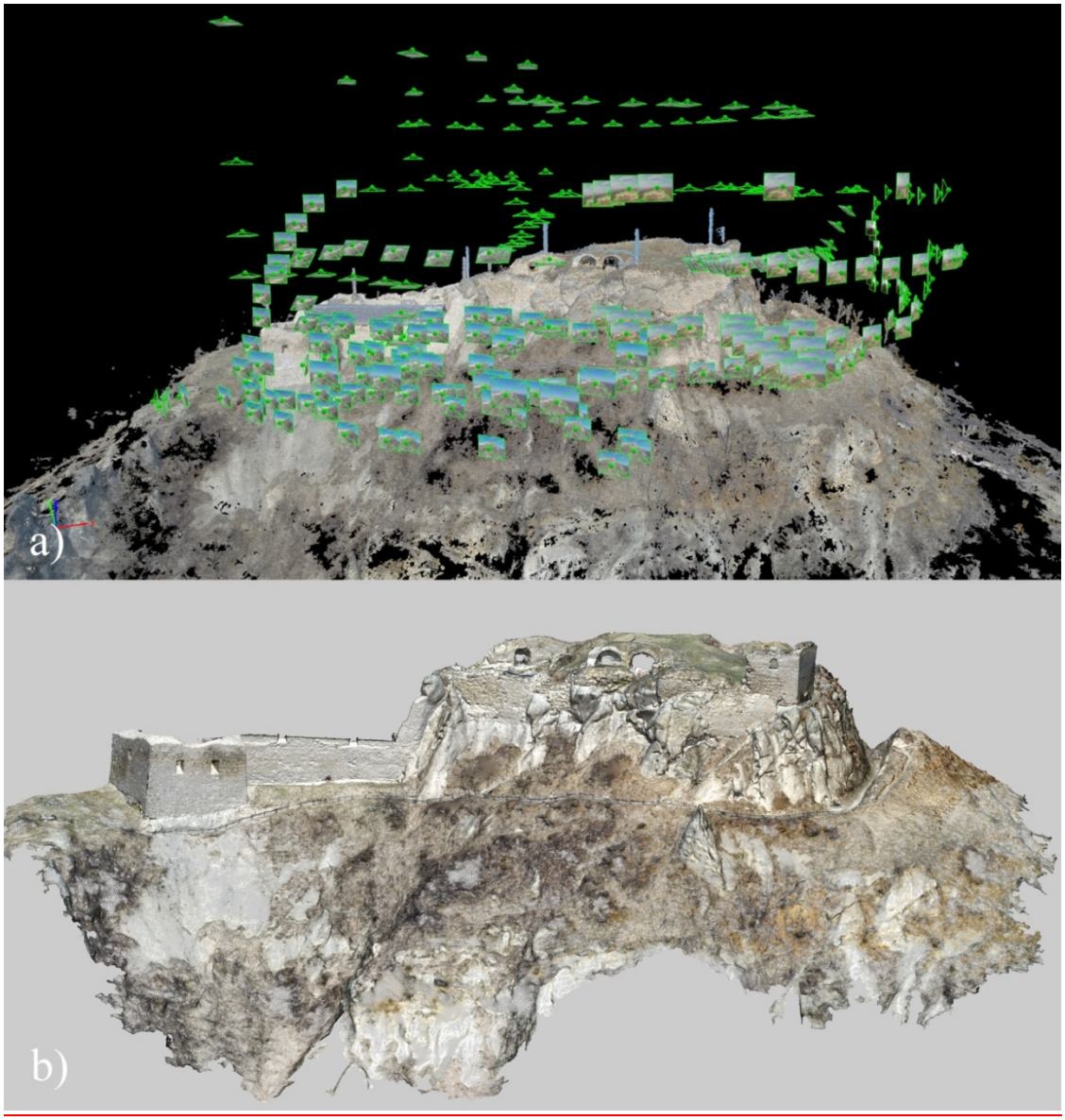

Fig.5. The captured image positions around the reconstructed castle hill (top) and the point clouds obtained by RPAS technology (bottom) (see top view on Fig. 3.)

~~Due to~~For georeferencing, particular tie objects ~~had to be~~were measured ~~also~~ by the Global Navigation Satellite System (GNSS). The used GNSS receiver was a Leica CS10 with a Gs08plus antenna (GS08, 2014, CS10, 2014). The measurement was done in RTK mode supported by the Hungarian RTK network (RTKnet, 2013). There were 7 measured ground control points (Fig. 6) (GCPs); the mean 3D measurement accuracy was 4.9 cm (minimal value was 2 cm, maximal value 9 cm). The RPAS technology has produced a considerable amount of data points (observations). Since this point cloud is difficult to manage due to its size, and heterogeneous point spacing, the latter processing requires a sophisticated resampling step, which was done by CloudCompare where the spatial resolution of the point cloud was set to 1 cm.

The RPAS data collection was validated by the use of terrestrial laser scanning. The necessary data were captured by two scanners~~,~~: a Faro Focus S 120 3D (Faro, 2016) and a Z+F Imager 5010C (Z+F 2014). The terrestrial laser scanning was executed on the same day as the RPAS mission. The raw point cloud measured by Faro scanner contained 1.9 billion points, whilst the Z+F point cloud had 0.8 billion points. Both point clouds ~~have~~included X, Y, Z coordinates, intensity and RGB ~~color~~colour values. RPAS and TLS based point clouds were compared by CloudCompare software (CloudCompare, 2014) (Fig. 7).

~~RPAS and TLS based point clouds could be compared by~~As one can notice in Fig. 7, the ~~software CloudCompare (CloudCompare, 2014) (Fig. 4).~~

~~The RPAS technology has produced considerable amount of points. Since this point cloud is difficult to be managed due to its size, and heterogeneous point spacing,~~highest difference between the ~~later processing requires a sophisticated resampling step, which was done by CloudCompare, where~~ two sources is almost less than 10 cm and the ~~spatial resolution~~majority of the ~~point cloud was set to~~differences is about 1 cm.

The point cloud was then imported into Geomagic Studio 2013 (GeomagicStudio, 2013) and meshed, where the triangle side length was 5-7 cm ~~(Fig. 7).~~ To support the engineering geological survey, several horizontal and vertical sections were derived in Geomagic DesignX 2016 (GeomagicDesignX, 2016); these profiles were exported in CAD-format ~~(Fig. 5).~~

The next step was to make cut-offs focusing only on the cliffs; it was done by CloudCompare, followed by the points being exported in LAS-format (LAS, 2012). The exported points could then be imported into SAGA GIS 2.1.2 (Conrad et al. 2015), where the necessary ~~DEMs~~DTMs were created by inverse distance weighting (IDW) algorithm (IDW, 2013). The derived ~~DEM~~DSM-grids have 5 cm spatial resolution, which is adequate for morphologic analyses (Fig. ~~4).~~6) and suits to slope stability analysis. The morphology analysis has concentrated on Catchment Area (CA) (Costa-Cabral and Burges 1994, Haas et al. 2016) (Fig 4), although several other morphological indices (e.g. Topographic Wetness Index, Stream Power Index) were derived ~~(Fig. 4).~~ These indices express the potential relationship between surface geometry and geological parameters.

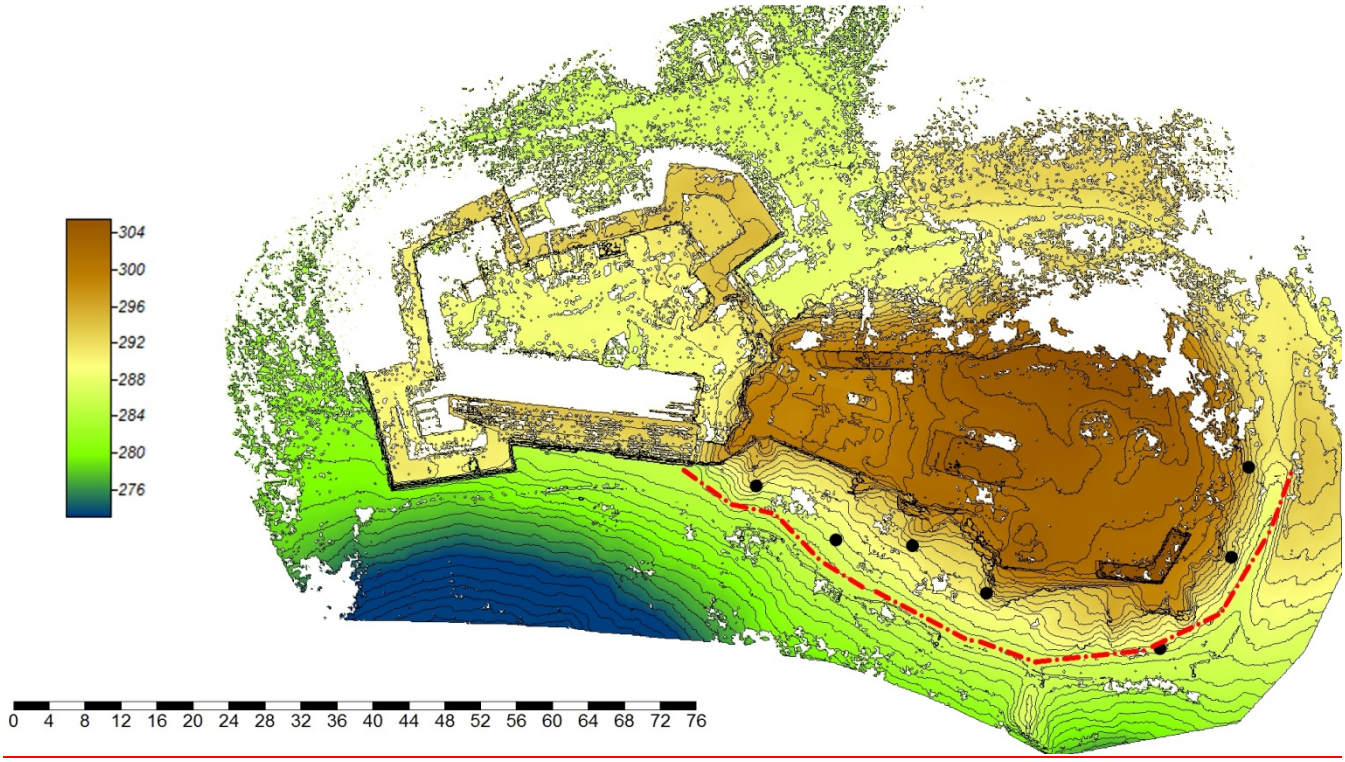

Fig.6. Colour Digital Surface Model with 1 m contour line interval of the study area. The solid black dots show the ground control points, while red dot-and-dash line represent zones affected by rock fall.

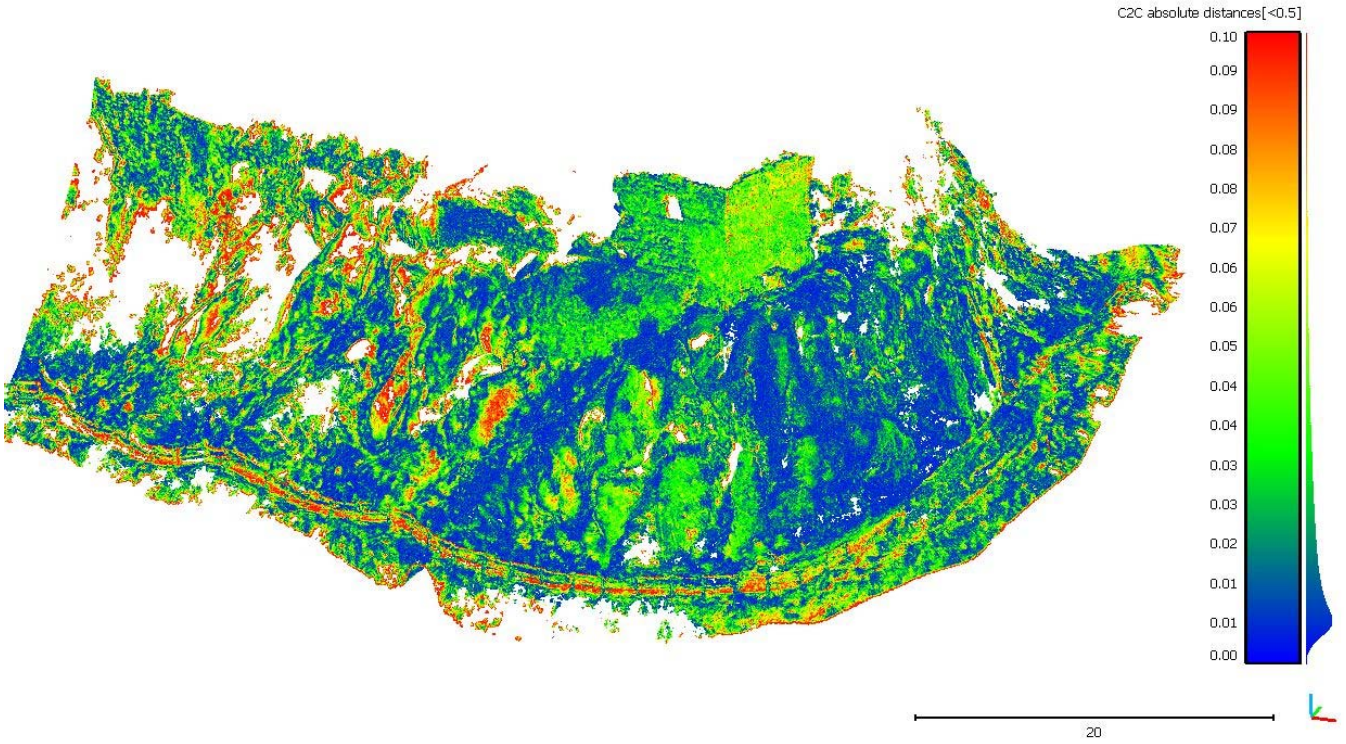

Fig. 7. Differences between RPAS and TLS point clouds by CloudCompare shown in metres (modus of differences is at about 0.01 m)

3.2 Engineering geology and slope stability analysis

Geological data and written resources (Balogh 1964, Haas 2013, Lukács et al. 2015) provided background information for the planning of engineering geological field survey (Fig. 4). Major lithotypes were identified and described and geological profiles were recorded during the engineering geological field surveys (Fig. 4). Rock joints, discontinuity surfaces, and fault systems were measured by using compass and structural geological software applied in mobile phone. The structural geological data was analysed by Dips software. Strength parameters were assessed on-site by using a Schmidt hammer. 10 rebound values were measured on each surface and mean values and standard deviations were also calculated. This method has been ~~also~~ used previously to gather rapid data on rock strength of cliff faces (Margottini et al. 2015). The data-set was compared to rock mechanical laboratory tests.

Samples for laboratory analyses were collected on site (Fig. 4). Major rock mechanical parameters were measured under laboratory conditions on cylindrical specimens. These were drilled from blocks and cut into by appropriate size using cutting disc. The sizes of tested specimen were made according to EN on air dry and on water saturated samples. The specimens were grouped according to the bulk density and the propagation speed of the ultrasonic pulse wave. Strength parameters such as uniaxial compressive strength, ~~an~~ indirect tensile strength (Brasilian), ~~was~~were measured according to relevant EN standards and ISRM suggested methods ~~and modulus~~. Modulus of elasticity was also calculated (Table ~~1~~2). The generalized Hoek-Brown failure criterion (Hoek et al. 2002) was used to determine strength parameters of the rock mass. Altogether, 53 cylindrical test specimens were used for the tests.

~~**Table 1. Rock mechanical tests and relevant standards.**~~

~~Rock mechanical parameter~~	~~Number of specimens~~	~~Relevant standard~~
~~Bulk density~~	~~53~~	~~EN 1936:2000~~

~~Water absorption~~	~~18~~	~~EN 13755:2008~~
~~Propagation speed of the ultrasonic wave~~	~~53~~	~~EN 14579:2005~~
~~Uniaxial compressive strength~~	~~31~~	~~ISRM 2015~~
~~Modulus of elasticity~~	~~31~~	~~ISRM 2015~~
~~Tensile strength (Brasilian)~~	~~23~~	~~ISRM 2015~~

The falling blocks can endanger the touristic footpath bellow the castle on the southern slopes~~;~~, therefore, the stability analysis of the rocky slopes was focused on this part of the cliff (Fig. 3). First, the rock mass failure was analysed with by the RocFall FEM software of the Rocscience (RS2). The steepest sections were determined from ~~to~~ the terrain model obtained from RPAS data. The GSI values of the rock masses were determined according to Marinos et al. (2005). The global stability of the hillslope of selected sections was calculated with RS2 software. Since the rhyolite tuff is a weak rock with few joints, the rock mass failure and the failure along discontinuities were also analysed. This kinematic analysis had been done with a stereographic tool. The orientations of main joint sets were obtained from ~~RPAS (DTM~~DSM model~~,~~ based morphological analyses with the use of Catchment Area tool. It assumes that major flow paths are related to joints, i.e. fracture system controls the drainage pattern (Costa-Cabaral et al. 1994). At~~Fig. 4) and at~~ accessible areas joints and fractures were also measured on site on the southern and south-eastern parts of the hillslope. Additional control field measurements were also made in the underground cellar system of the castle, where the tuff is also exposed. The Dips software was used for the kinematic analysis. The direction of the hillslopes and the direction of the discontinuities were compared to determine the location of the potential hazardous failure zones on the hillside. Stereographic plots were generated showing the possible failure planes for all slope directions and the safety factor of the possible planar failure was calculated by ~~Roeplane~~Rockplane software. Wedge failure was modelled by Swedge software. Toppling failure due to geological and geomorphological conditions cannot occur. ~~Risk assessment was based on slope~~Slope stability calculations and stability assessment formed the last part of the engineering geological analyses (Fig. 4).

Table 2. Rock mechanical tests and relevant standards.

Rock mechanical parameter	Number of specimens	Relevant standard
Bulk density	53	EN 1936:2000
Water absorption	18	EN 13755:2008
Propagation speed of the ultrasonic wave	53	EN 14579:2005
Uniaxial compressive strength	31	ISRM 2015
Modulus of elasticity	31	ISRM 2015
Tensile strength (Brasilian)	23	ISRM 2015

4. Results

The rhyolite tuff faces consist of moderately bedded ignimbritic horizons, and also brecciated lapilli tuffs and tuffs according to our field observations (Fig. 6). The topmost 10 metres of the cliff face, which was modelled from slope stability, comprises 3 main horizons and can be modelled as “sandwich structure”. The lower and the upper ~~part~~parts are formed by thick pumice containing lapilli tuffs. These beds enclose nearly 2 metres of well-bedded less-welded fine tuff and brecciated horizons (Fig. ~~6~~8).

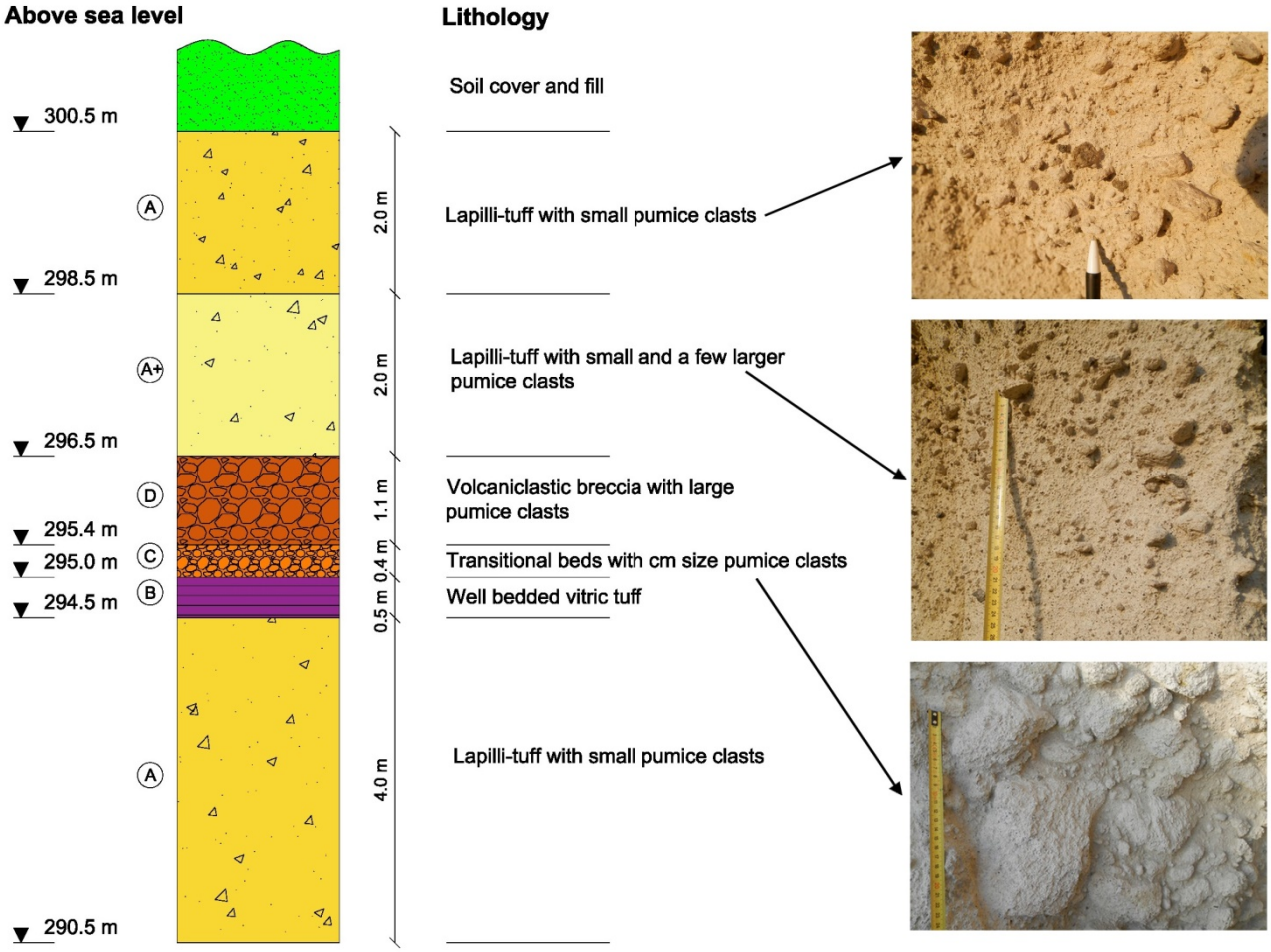

Fig.~~6~~8. Lithologic column of Sirok Várhegy showing the modelled topmost 10 metres section of the hill (letters refer to lithologic units)

Combining and comparing all measured data of discontinuities and joints, using ~~DTM~~DSM and its derivative of (Fig 6.) and morphological index (Fig. ~~4~~9) the joint orientation was outlined. The filed survey validated the obtained structural geological conditions ~~were clarified:~~and six main joint sets (with dip angle/dip directions of: 85/156, 88/312, 79/110, 81/089, 82/064, 61/299) were identified with prevailing NE – SW direction ~~(Fig. 7).~~.

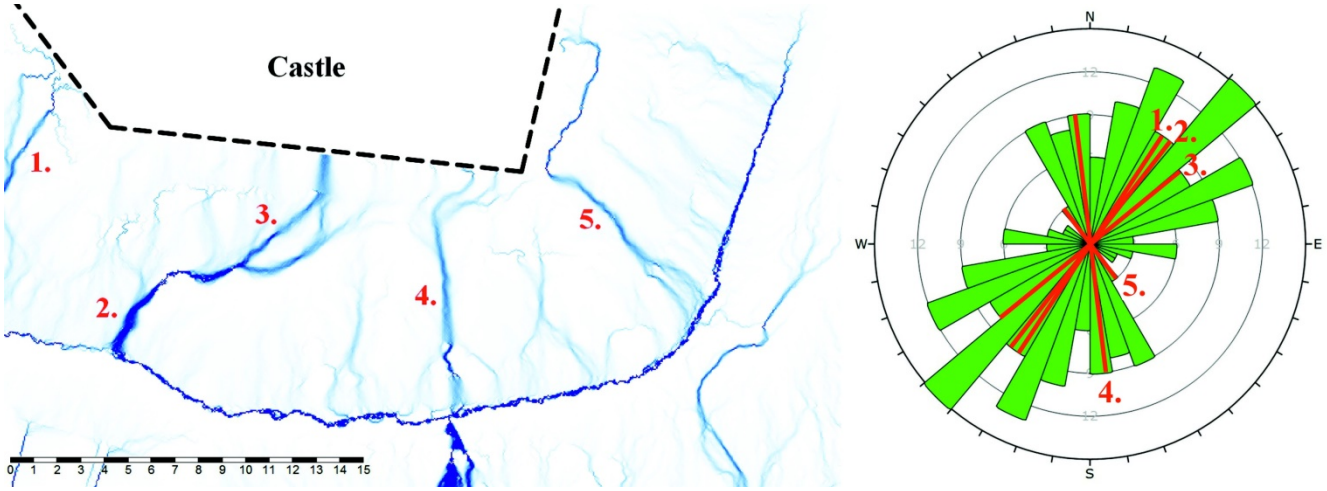

Fig.~~7~~9. Top view of the cliff (see the location on Fig. 3) obtained with RPAS and the catchment area diagram obtained from ~~DEM~~DSM analysis ~~(Fig. 4) that~~by using Catchment Area module (Costa-Cabral et al. 1994). The latter one was used for joint pattern recognition. Numbers refer to major joint systems marked on ~~DEM~~catchment area map and on rose diagram of the field measurements and ~~RPAS~~DSM data set.

The laboratory tests of tuffs provided the input data for stability analysis for the two main lithologies: upper and lower unit of lapilli tuff and middle unit of less welded tuff (Table ~~2~~3). In the model calculations GSI=50 value was used.

Table ~~2~~3. Rock mechanical parameters of tuff used in the model: lapilli tuff refers to upper and lower 4 metres, less welded tuff refers to middle stratigraphic unit

Mechanical property		Upper and Lower unit (marked by A on Fig. 10) (Lapilli tuff)	Middle unit (marked by B-D on Fig. 10) (Less welded tuff)

Bulk density(ρ)	[kg/m^3]	1815	1635
Uniaxial compressive strength(σ_c)	[MPa]	8.02	0.35
Tensile strength (σ_t)	[MPa]	0.83	0.04
Modulus of elasticity(E)	[GPa]	0.97	0.05

The results of RS2 FEM analyses suggest that the global factor of safety is SRF=1.27-1.71 in the studied sections (~~see~~ some of the selected sections are shown on Fig ~~4).~~3). The aim of the analysis is to determine the critical strength reduction factor (SRF) that can be considered the safety factor of the slope (Fig. 10). The SRF factor is influenced by the weak tuff layer (marked by B-D on Fig. ~~6)~~8), which has very low shear strength compared to the lapilli tuff. Colours on Fig. 10. represent the total displacements as a result of the shear strength reduction analysis (Rocscience, 2017). Thus these are not real displacements of the hillslope. The figure demonstrates only how the failure of the slope would occur with reduced shear strength parameters. Our failure analyses have ~~demonstrated~~proved that the bottom of the slip surface would be in ~~the~~this weaker layer ~~(marked by B-D on Fig. 8)~~ and could lead to a larger mass movement.

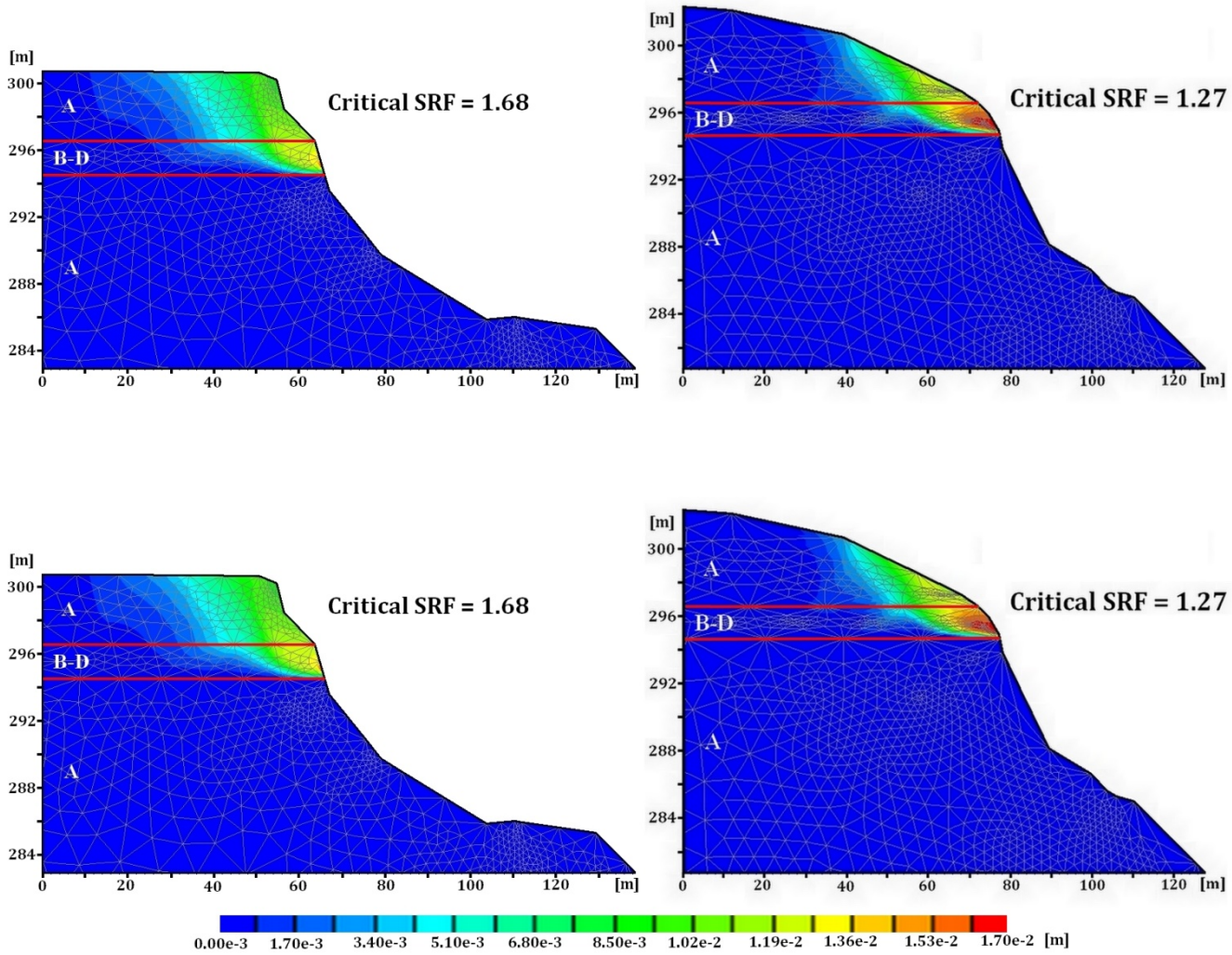

Fig.~~8~~10. The results of the global stability analysis of the slopes (sections 3 and 4 on Fig. 3), total displacements are marked in blue to red (lithology is indicated by letters A-D, note the weak zone marked by B-D, description of lithologies is given on Fig.~~6~~8.)

Other failure modes that were studied are planar failure and wedge failure, which are often controlled by joints and discontinuities. According to ~~DTM joint analyses (Fig. 7)~~data obtained from remote sensing and according to field ~~recordings~~measurements there was no ~~regular~~uniform spacing of the discontinuities. Stereographic plots with possible failure

planes for all slope directions (Fig. ~~9~~11) indicate that the most hazardous part of the slope is the one where the plane orientation is 75/75. The calculated factor of safety (FS= 1.15) implies high probability of planar failure.

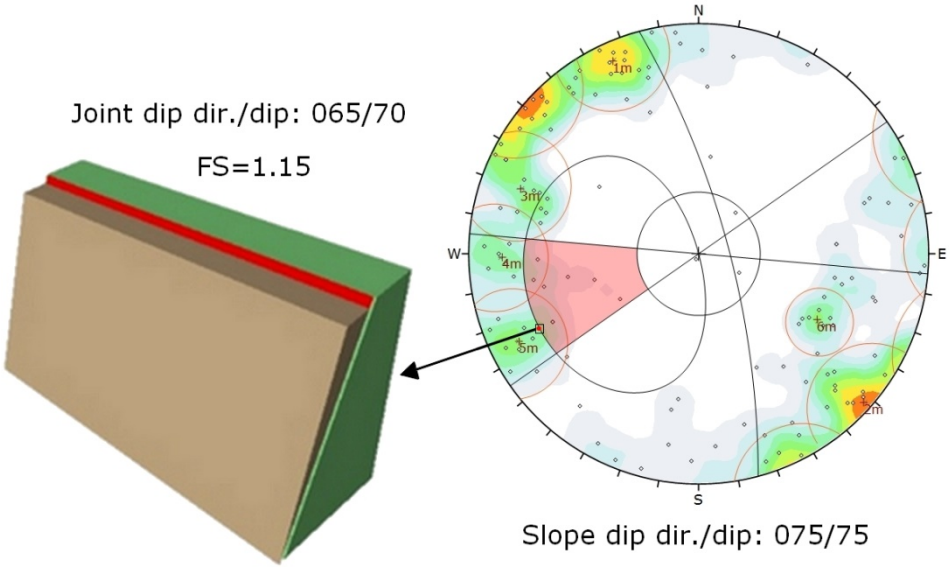

Fig.~~9~~11. Kinematic analysis of planar failure by Rockplane (main joint sets are marked by red circles 1m-6m)

Three possible wedge failure modes were identified as being the most hazardous, according to our calculations by Swedge software (Fig. ~~10~~12). In these three cases the factor of safety was in the range of 1.38-1.94 representing the hazards of rock falls along wedges delineated by different joint systems.

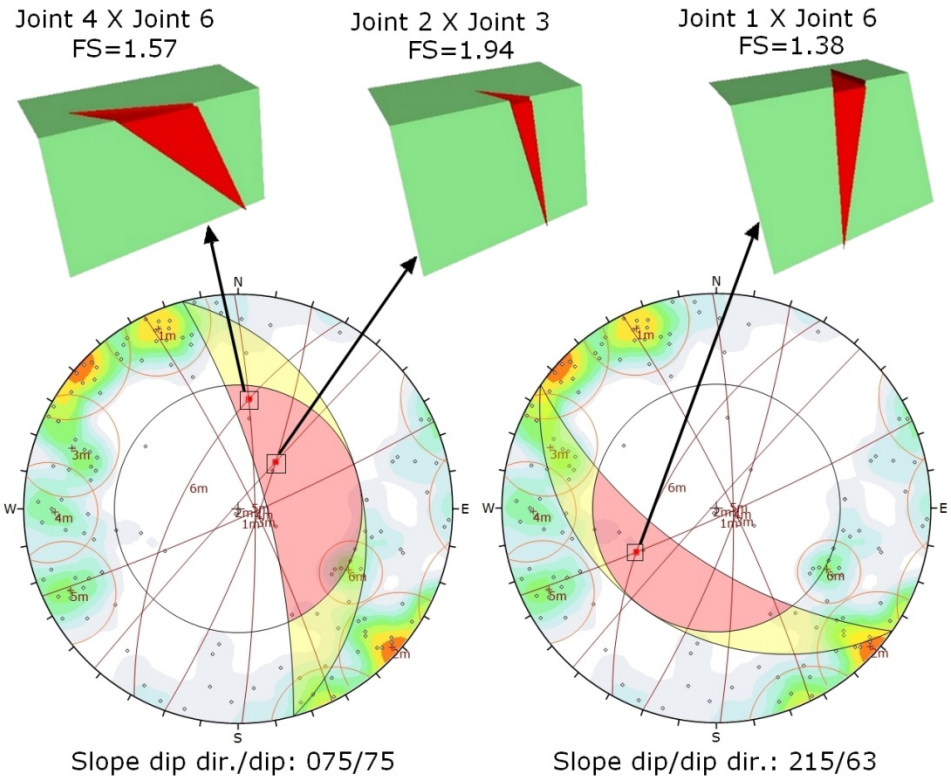

Fig.~~10~~12. Examples for the kinematic analysis of wedge failures (main joint sets are marked by red circles 1m-6m)

5. Discussion

There are three critical sets of input data in the modelling of rocky slopes: i) terrain model and slope geometry, ii) joints system and iii) strength of rock mass.

To obtain the first, the slope geometry, RPAS ~~based surveying technique was used, because even the hardly accessible cliffs could be surveyed with this method (Giordan et al. -~~-based surveying technique was used similarly to previous studies (Giordan et al. 2015). In many previous studies RPAS mission was performed following a flight plan (Eisenbeiss 2008, Lindner et al. 2016). In our case no flight plan was made prior to mission, and the windy conditions were also not favourable for pre-programmed flight route. The flight was manually controlled and the skilled personnel with a First-Person Viewer tool controlled the image acquisition. The crucial points were the necessary overlaps of images and the matching. The overlaps were ensured by three consequent flights around the study area that provided a dense network of image acquisition locations (Fig. 5). The obtained 1174 images covered the entire study area with appropriate overlaps. The number of images is reasonable, since in previous studies 400 images were taken for a smaller translational rockslide by a GoPro Hero 3 Black camera (Tannant et al. 2017) or app. 400-900 images with a higher resolution camera (18MP) for a landslide area that is approximately five times larger than this one (Lindner et al. 2016). The Pix4Dmapper software (SfM) was used to identify keypoints. Nearly 10,000 keypoints were found on each image (Table 1), which is considered a sufficient amount to provide appropriate matching (Remondino et al. 2014). Camera self-calibration tool and rolling shutter effect correction were the other key features of this software that allowed the processing the images of GoPro Hero 3+ camera. The obliquity of images (Rupnik et al. 2014) and the density of obtained data (Remondino et al. 2014, Rupnik et al. 2015) are crucial in the applicability and accuracy of these images. These were also manged by Pix4Dmapper. The GNNS system and the ground control points (Fig. 6) allowed to georeferencing of the rocky slope. Our results show that the mean 3D accuracy was 4.9 cm. It is comparable with the ground resolution of 1-3.5 cm/pixel of Italian rockslide survey (Tannant et al. 2017), or 3.3-4.1 cm (Neugirg et al. 2016). This resolution was appropriate to create a reliable Digital Surface Model.

RPAS-based data was also validated with TLS measurements. The co-use of these remote sensing tools has been previously well-documented for other applications such as soil roughness (Milenkovich et al. 2016) in erosion detection (Neugirg et al. 2016) or in cultural heritage (Eisenbeiss & Zhang 2006). The RPAS obtained data validation was performed by comparing the two point clouds obtained by RPAS and TLS. The surfaces were resampled~~2015). RPAS based data had to be validated. TLS measurements were used for this, in a way that the two point clouds covering the surface were resampled,~~ in order to homogenize the spatial resolution. The point densities have been tested in CloudCompare, as a unit sphere of volume of 1 m^3 was defined where the points can be counted and then the sphere can be moved along the whole surface. The differences in point clouds are less than 10 cm (Fig 7), which is considered a reasonably good match in terrain modelling (Neugirg et al. 2016). This computation proved that the average point density in both point clouds are practically the same, although the RPAS densities are more homogeneous, while the TLS has denser point clouds close to the scanning stations~~.~~, as it was expected on the basis of previous works (Naumann et al. 2013)

Another aspect causing some differences between the two data sets is that the image based reconstruction is performed by interest operators, very usually SIFT (Scale-invariant Feature Transform) or similar computer vision operators (Lowe 2004). These operators are generally sensitive to intensity jumps, points, or corners, and textural changes in the input images. If the image resolution is not adequate or the object is locally “smooth”, these operators do not return with surface points and the output of the reconstruction has some “filtered” effect. Fortunately, the surface reconstruction quality in RPAS processing resulted minor, ignorable smoothing ~~effect~~effects. Comparing the two data sets, it is clearly proven that the geometric resolution of the RPAS-based digital ~~elevation~~surface model corresponds to the TLS one, offering ~~the same~~very similar quality ~~level as~~data (Fig.7). It is necessary to note that vegetation can hamper TLS measurements (Prokop & Panholzer 2009, Scaioni et al. 2014, Tannant 2015) and thus limit the comparison of RPAS and TLS obtained data (Milenkovic et al.

2016). In our case most of the ~~terrestrial laser scanning.~~study area was bare and if vegetation occurred manual removal was made.

The documentation of joint system and ~~discontinuity surfaces based on field~~discontinuities are crucial for rock wall stability assessment (Tannant et al. 2017). Field survey ~~provided~~can only provide reliable data on joint orientation~~;~~ of accessible areas (Margottini et al. 2015); however, the joint system that was found on inaccessible cliffs was not detectable. To overcome this problem, RPAS generated images were used; the frequency of joints was observed based on these images like in previous studies by Assali et al. (2014), Martino & Mazzanti (2014) and Margottini et al. (2015). The required resolution for joint frequency is in the order of 10 cm, rarely 1 cm~~.~~ (Tannant 2015, Tannant et al. 2017). The RPAS technique allows ~~having~~for plane surface geometries, however, many joints are not plane surfaces and there are ~~hardly visible~~ sets in shadows~~.~~ that are difficult to visualize. Thus, RPAS can be used to outline the strike of major joints, but it might ~~causes problem~~cause problems when it comes to the determination of dip and the displacement along the fault planes (e.g. slickensides).

~~For the determination of the strength of rock masses, we first used Schmidt hammer on site, which is a common practice (Margottini et al. 2015).~~ Our field tests indicate that the application of Schmidt hammer in rock strength analysis is limited when it comes to the analysis of low strength rocks, such as volcanic tuff (Aydan & Ulusay 2003). As a consequence, laboratory analyses of samples were also required to obtain reliable strength parameters. To measure the strength and to understand the weathering characteristics, samples were taken, representing different stratigraphic positions. Our lab test data (Table ~~2~~3) clearly indicates that a low strength unit is found in the studied sections (unit marked by 'B-D' on Fig 8). Whether the low strength of this zone is related to differential weathering (Török et al. 2007), or it is associated with inherited weakness (micro-fabric~~)~~), is not clear. This layer is a potential failure zone as it was shown by slope stability calculations. Similar intercalation of pumice-rich layered deposits was modelled by Damiano et al. (2017). They found that a pumice-reach weak zone is prone to rainfall induced landslides. Our results are in good correlations with ~~the previous~~these findings since ~~this~~the studied rhyolitic volcanic tuff was also proved to be very prone to weathering. A loss in tensile strength of 60% was measured under simulated laboratory conditions (Stück et al. 2008). Weathering processes have been long known to induce landslides and cause slope stability problems in various lithologies and especially pyroclastic rocks (Chigra 2002, Fanti et al. 2013). At the studied rhyolite tuff cliff face, it was shown that joint system is responsible for slope instabilities: planar and wedge failures were found (Fig. ~~9., Fig. 10). It is in agreement in several previous works, where the structural geological control of slope stability of highly dissected cliffs was pointed out (Agliardi et al. 2013, Fanti et al. 2013, Feng et al.~~ 11., Fig. 12). These failure modes are common in hard jointed cliff faces (porphyry Agliardi et al. 2013, mica-schist Tannant et al. 2017, limestone Feng et al. 2014). Our study demonstrates that joint system has an important control on slope stability not only in hard rock lithologies but also in weak tuffs. It is in the line with Fanti et al. 2013 and Margottini 2015, since in Italy and in Giorgia rock walls of volcanic tuffs suffered landslides. The kinematic analysis of tuff rock walls of Tuscany (Fanti et al. 2013) also demonstrated that wedge failure and planar failure are the most common failure mechanisms of tuff cliff faces.~~2014).~~

~~Comparison of surveying techniques obtaining of slope geometry and terrain model data for slope stability analysis helps to choose the appropriate technique (Table 3).~~

~~The professional routine is mostly required for classical tachymetry, where the surveyors need to have geological knowledge and surveying expertise to collect the most relevant points. This technology operates usually by the lowest number of measured points, so their quality and distribution is therefore very crucial. The TLS of nowadays are in counterpart very fast instruments (Assali et al. 2014, Neugrig et al. 2016) capturing high amount of terrain points with the ease like using smart phones. Image capture by RPAS is fairly easy; time dependent automatic image capture (e.g. shoot in every second) allows to obtain reliable data. These cameras are mostly equipped by automatic exposure control, which are similar to pocket camera use. One of the drawbacks is that flying requires expertise in flight planning and/or manual operator control. Thanks~~

~~to onboard electronics, the fastest data capturing method is the RPAS based. This feature is advantageous if the object availability is limited or the objects are moving/changing. Surveying is the slowest solution to acquire the points, but the data processing is similarly fast (Table 3). TLS and RPAS collected data oblige more processing time – sometimes it is computational hardware dependent. The most homogenous data is obtained by the RPAS methodology; tachymetry can be applied also in this manner, although the efficiency is then very poor (Table 3). TLS has a typical circular pattern having decreasing point density. By corresponding resampling and/or interpolation this drawback can be eliminated. The highest spatial resolution can be achieved by TLS (Table 3). The spatial resolution of RPAS depends on flying time and object distance. Tachymetry is generally a low resolution data collection way. Because tachymeters and laser scanners must stand on the terrain, these technologies are highly dependent from terrain accessibility (slope steepness, vegetation), which is very advantageous for RPAS based technology (Table 3). RPAS is similarly very robust on shadowing effects, caused by vegetation or other objects. The cost estimations for the given technologies were compiled by the experience taken from the literature. Excellent comparisons and evaluations can be found in Eisenbeiss & Zhang 2006, Koma et al. 2014, Milenkovic et al 2016, Naumann et al. 2013, Rothmund et al. 2013. The data set suggests that on average the costs of RPAS survey are lower than that of TLDS and tachmietry (Table 3).~~

~~**Table 3. Comparison of the applicability of RPAS-based technology with terrestrial laser scanning (TLS) and tachymetry for rock slope stability assessment. Time frames and applicability is marked by '+' while costs are shown by '$'**~~

	~~RPAS~~	~~TLS~~	~~Tachymetry~~
~~Required expertise~~	~~++~~	~~+~~	~~+++~~
~~Data capturing speed on site (number of obtained data points)~~	~~+++~~	~~++~~	~~+~~
~~Required data processing time~~	~~++~~	~~++~~	~~+~~
~~Homogeneity of collected data~~	~~+++~~	~~++~~	~~+/++/+++~~
~~Resolution~~	~~++~~	~~+++~~	~~+~~
~~Difficulty caused by slope accessibility~~	~~+~~	~~++~~	~~++~~
~~Digital terrain modelling~~	~~+++~~	~~+++~~	~~+~~
~~Slope geometry~~	~~+++~~	~~+++~~	~~++~~
~~Joint system detection~~	~~+++~~	~~+++/++~~	~~+~~
~~Costs of surveying~~	~~$~~	~~$$~~	~~$$$~~
~~Costs of data processing~~	~~$$~~	~~$$~~	~~$~~

~~+ low, ++ medium, +++ high, $ low, $$ medium, $$$ high~~

6. Conclusions

- The ~~use~~manually controlled flights of RPAS ~~technique can overcome the bottleneck of detecting the geometries~~provided excellent information on slope geometry of highly dissected and inaccessible slopes. ~~RPAS equipped~~

- The necessary overlap between images was ensured by three flights over the small area, by the skilled personnel using First-Person Viewer system with ~~camera provides relevant amount and quality of imagery~~a synchronous image transfer.

- The obtained data ~~on steep cliff faces.~~ were manged by Pix4Dmapper (SfM) software allowing the identification of nearly 10.000 keypoints per image.

~~- Comparing with TLS and tachimetry RPAS technique is much safer; cheaper, faster and provides excellent terrain model after data processing.~~

~~- Documentation of joints is essential for cliff face stability analysis. RPAS~~ The TLS based point clouds proved to be good tools to validate the accuracy of images and data sets of manually controlled RPAS. In our study the maximum difference between the two point clouds were less than 10 cm, but mostly around 1 cm.

- RPAS collected images and the point cloud based Digital Surface Model and especially Catchment Area method allows the detection of joint system (mainly strikes and partly dips but not slickensides) but field validation and field measurements of accessible joints and faults are recommended to justify joint orientation ~~obtained from RPAS data based terrain models~~.

- The obtained digital surface model was accurate enough to allow complying cross-sections for rock wall stability calculations.

- The lithology and physical parameters of the studied steep cliffs are not uniform and intercalations of weak layers of vitric tuff and volcanoclastic breccia were found.

- According to 2D FEM modelling the intercalating low strength layer is the one where potential slip surface can develop causing larger scale mass movements, but at present it has low probability.

- Joint system has a crucial role in the stability of the studied rhyolite tuff cliff faces. The highest hazard is related to planar failure along ENE-WSW joints and to wedge failure.

Acknowledgements

The help of B. Czinder, B. Kleb, Z. Koppányi, B. Molnár, B. Pálinkás and B. Vásárhelyi is acknowledged. The ~~support of~~research was supported by the National Research Development and Innovation Fund (NKFI) ~~Fund~~ (ref. no. K 116532~~) is~~). The constructive comments of the anonymous reviewers are appreciated.

References

Abbruzzese, J. M., Sauthier, C., Labiouse, V.: Considerations on Swiss methodologies for rock fall hazard mapping based on trajectory modeling. Nat. Hazards Earth Syst. Sci., 9, 1095–1109, doi:10.5194/nhess-9-1095-2009, 2009.

Agliardi, F., Crosta, G.B., Meloni, F., Valle, C., and Rivolta, C.: Structurally-controlled instability, damage and slope failure in a porphyry rock mass, Tectonophysics 605 (2013) 34–47, doi:10.1016/j.tecto.2013.05.033, 2013.

Arikan, F., Ulusay, R. and Aydin, N.: Characterization of weathered acidic volcanic rocks and a weathering classification based on a rating system. Bulletin of Engineering Geology and the Environment, 66 (4): 415-430, 2007. doi:10.1007/s10064-007-0087-0, 2007.

Assali, P., Grussenmeyer, P., Villemin, T., Pollet, N. and Viguier, F.: Surveying and modelling of rock discontinuities by terrestrial laser scanning and photogrammetry: Semi-automatic approaches for linear outcrop inspection. J. of Struct. Geol., 66: 102-114, doi:10.1016/j.jsg.2014.05.014, 2014.

Aydan, Ö., and Ulusay, R.: Geotechnical and environmental characteristics of man-made underground structures in Cappadocia, Turkey. Eng. Geol., 69 (3/4): 245-272, doi:10.1016/S0013-7952(02)00285-5, 2003.

Balogh K.: Geological Formations of Bükk Mountains (in Hungarian), Annual Report of the Hungarian Geological Survey, 48(2), 245-719 1964.

Brauneck, J., Pohl, R., Juepner, R.: Experiences of using UAVs for monitoring levee breaches. IOP Conf. Series: Earth and Environmental Science 46, 012046, IOP Publishing, doi:10.1088/1755-1315/46/1/012046, 2016.

Budetta, P.: Assessment of rockfall risk along roads, Nat. Hazards Earth Syst. Sci., 4, 71–81, doi:10.5194/nhess-4-71-2004, 2004.

Casella, E., Rovere, A., Pedroncini, A., Stark, C. P., Casella, M., Ferrari, M., Firpo, M.: Drones as tools for monitoring beach topography changes in the Ligurian Sea (NW Mediterranean), Geo-Marine Letters, 36(2), 151-163., doi:10.1007/s00367-016-0435-9, 2016.

Chigira, M.: Geologic factors contributing to landslide generation in a pyroclastic area: August 1998 Nishigo Village, Japan, Geomorphology, Vol. 46(1-2~~),~~): 117-128, doi:10.1016/S0169-555X(02)00058-2, 2002.

Civera, J., Davison A.J., Martínez Montiel J.M.: Structure from Motion Using the Extended Kalman Filter. Springer Tracts in Advanced Robotics. DOI: 10.1007/978-3-642-24834-42012, pp 1-172, 2012.

Cloud Compare point cloud processing software (CC) available at: http://www.cloudcompare.org/ (last access 1 February 2017), 2014

Conrad, O., Bechtel, B., Bock, M., Dietrich, H., Fischer, E., Gerlitz, L., Wehberg, J., Wichmann, V., and Böhner, J.: System for Automated Geoscientific Analyses (SAGA) v. 2.1.4, Geosci. Model Dev., 8, 1991-2007, doi:10.5194/gmd-8-1991-2015, 2015.

Copons, R., Vilaplana, J. M., and Linares, R.: Rockfall travel distance analysis by using empirical models (Solà d'Andorra la Vella, Central Pyrenees), Nat. Hazards Earth Syst. Sci., 9~~,~~: 2107-2118, doi:10.5194/nhess-9-2107-2009, 2009.

Costa-Cabral, M.C., Burges, S.J.: Digital Elevation Model Networks (DEMON): a model of flow over hillslopes for computation of contributing and dispersal areas, Water Resources Research, 30: 1681-1692, doi: 10.1029/93WR03512, 1994.

Crosta, G, and Agliardi, F.: How to obtain alert velocity thresholds for large rockslides. Phys Chem Earth Parts ABC. 27~~:~~, 1557-1565, doi:10.1016/S1474-7065(02)00177-8, 2002.

Crosta, G. B., and Agliardi, F.: A methodology for physically based rockfall hazard assessment. Natural Hazards and Earth System Sciences 3: 407–422, doi:10.5194/nhess-3-407-2003, 2003.

Damiano, E., Greco, R., Guida A., Olivares, L., Picarelli, L.: Investigation on rainwater infiltration into layered shallow covers in pyroclastic soils and its effect on slope stability. Engineering Geology 220: 208–218, https://dx.doi.org/10.1016/j.enggeo.2017.02.006, 2017.

Danzi M., Di Crescenzo G., Ramondini M., Santo A. Use of unmanned aerial vehicles (UAVs) for photogrammetric surveys in rockfall instability studies, Rend. Online Soc. Geol. It., Vol. XX, doi: 10.3301/Rol.2012.xx, 2013.

De Biagi, V., Napoli, M.L., Barbero, M., and Peila, D.: Estimation of the return period of rockfall blocks according to their size. Nat. Hazards Earth Syst. Sci., 17, 103–113, 2017, doi:10.5194/nhess-17-103-2017, 2017.

DJI phantom 2 quadrocopter (DJI) available at: http://www.dji.com/phantom-2 (last access 1 February 2017), 2015.

Eisenbeiss, H. The autonomous mini-helicopter: A powerful platform for mobile mapping. International Archives of the Photogrammetry, Remote Sensing and Spatial Information Sciences. 37/B1, 977–983, 2008.

Eisenbeiss, H., Zhang, L. ~~(2006):~~ Comparison of DSMs generated from mini UAV imagery and terrestrial laser scanner in a cultural heritage application, International Archives of the Photogrammetry, Remote Sensing and Spatial Information Sciences, Volume XXXV/5~~, pp.~~: 90-96, 2006.

Fanti, R., Gigli, G., Lombardi, L., Tapete, D., Canuti, P., Terrestrial laser scanning for rockfall stability analysis in the cultural heritage site of Pitigliano (Italy). Landslides 10:409–420, DOI 10.1007/s10346-012-0329-5, 2013.

Faro terrestrial laser scanner (Faro) available at: http://www.faro.com/en-us/products/3d-surveying/faro-focus3d/overview (last access 1 February 2017), 2016.

Feng, Z., Li, B., Yin, Y. P., and He, K.: Rockslides on limestone cliffs with subhorizontal bedding in the southwestern calcareous area of China. Nat. Hazards Earth Syst. Sci., 14, 2627-2635, doi:10.5194/nhess-14-2627-2014, 2014.

Feng, Q., Liu, J. and Gong, J.: Urban Flood Mapping Based on Unmanned Aerial Vehicle Remote Sensing and Random Forest Classifier—A Case of Yuyao, China, Water, 7(4), 1437–1455, doi:10.3390/w7041437, 2015.

Francioni, M., Salvini, R., Stead, D., and Litrico, S.: A case study integrating remote sensing and distinct element analysis to quarry slope stability assessment in the Monte Altissimo area, Italy. Eng. Geol., 183: 290-302., doi:10.1016/j.enggeo.2014.09.003, 2014.

Fraštia, M., Marčiš, M., Kopecký, M., Liščák, P., Žilka, A.: Complex geodetic and photogrammetric monitoring of the Kraľovany rock slide. Journal of Sustainable Mining, 13(4), 12–16. doi: 10.7424/jsm140403, 2014.

Geomagic Design X 3D modelling software (GeomagicDesignX) available at: http://www.geomagic.com/en/products-landing-pages/designx (last access 1 February 2017), 2016

Geomagic Studio 3D modelling software (GeomagicStudio) available at: http://www.geomagic.com/en/ (last access 1 February 2017), 2013

Gerke, M. and Kerle, N.: Automatic structural seismic damage assessment with airborne oblique pictometry imagery. Photogrammetric Engineering and Remote Sensing, 77(9) pp. 885-898, doi: 10.14358/PERS.77.9.885 2011.

Giordan, D., Manconi A., Allasia P., and Bertolo D.: Brief Communication: On the rapid and efficient monitoring results dissemination in landslide emergency scenarios: the Mont de La Saxe case study. Nat. Hazards Earth Syst. Sci., 15, 2009–2017, 2015, oi:10.5194/nhess-15-2009-2015, 2015.

GoPro action cam (GoPro) available at: https://gopro.com/ (last access 1 February 2017), 2017

Haas J.: Geology of Hungary, Springer, Berlin, 1-246, doi: 10.1007/978-3-642-21910-8, 2013.

Haas, F., Hilger, L., Neugirg, F., Umstädter, K., Breitung, C., Fischer, P., Hilger, P., Heckmann, T., Dusik, J., Kaiser, A., Schmidt, J., Della Seta, M., Rosenkranz, R., and Becht, M.: Quantification and analysis of geomorphic processes on a recultivated iron ore mine on the Italian island of Elba using long-term ground-based lidar and photogrammetric SfM data by a UAV, Nat. Hazards Earth Syst. Sci., 16~~,~~: 1269-1288, doi:10.5194/nhess-16-1269-2016, 2016.

Hoek, E., Carranza-Torres, C., and Corkum, B.: Hoek-Brown failure criterion – 2002 Edition. Proc. NARMS-TAC Conference, Toronto, 1, 267-273, 2002.

Inverse distance weighting interpolation (IDW) available at: http://gisgeography.com/inverse-distance-weighting-idw-interpolation/ (last access 1 February 2017), 2013

Jovančević, S. D., Peranić, J., Ružić, I. and Arbanas, Ž.: Analysis of a historical landslide in the Rječina River Valley, Croatia. Geoenvironmental Disasters, 3:26, doi:10.1186/s40677-016-0061-x, 2016.

Kleb B, Vásárhelyi, B.: Test results and empirical formulas of rock mechanical parameters of rhiolitic tuff samples from Eger's cellars. Acta Geologica Hungarica 46(3): 301-312, https://doi.org/10.1556/AGeol.46.2003.3.5, 2003.

Koma, Zs., Székely, B., Dorninger, P., Rasztovits, S., Roncat, A., Zámolyi, A., Krawczyk, D., Pfeifer, N. (2014): Comparison of UAV and TLS DTMs for acquisition of geological, geomorphological information for Doren landslide, Vorarlberg Austria, EGU General Assembly Conference Abstracts, 2014

LAS laser scanner point cloud datatype specification (LAS) available at: https://www.asprs.org/committee-general/laser-las-file-format-exchange-activities.html (last access 1 February 2017), 2012

Leica CS10 controller (CS10) available at: http://leica-geosystems.com/products/gnss-systems/controllers/leica-viva-cs15-and-cs10 (last access 1 February 2017), 2014

Leica Cyclone point cloud processing software (LeicaCyclone) available at: http://leica-geosystems.com/products/laser-scanners/software/leica-cyclone (last access 1 February 2017), 2016

Leica GNSS receiver (GS08) available at: http://leica-geosystems.com/products/gnss-systems/smart-antennas/leica-viva-gs08plus (last access 1 February 2017), 2014

Lindner, G., Schraml, K., Mansberger, R., Hübl J. UAV monitoring and documentation of a large landslide. Appl Geomat 8:1–11, DOI 10.1007/s12518-015-0165-0, 2016.

Lowe, D.G~~. (2004).~~.: Distinctive Image Features from Scale-Invariant Keypoints. International Journal of Computer Vision 60: 91-110, doi: 10.1023/B:VISI.0000029664.99615.94, 2004.

Lukács R, Harangi S, Bachmann O, Guillong M, Danišík M, Buret Y, von Quadt A, Dunkl I, Fodor L, Sliwinski J, Soós I, Szepesi J.: Zircon geochronology and geochemistry to constrain the youngest eruption events and magma evolution of the Mid-Miocene ignimbrite flare-up in the Pannonian Basin, eastern central Europe. Contributions to Mineralogy and Petrology. 170: 1-26, doi:10.1007/s00410-015-1206-8, 2015.

Manconi, A., and Giordan, D.: Landslide failure forecast in near-real-time, Geomatics, Natural Hazards and Risk, ~~2014,~~ doi:10.1080/19475705.2014.942388, 2014.

Manconi, A., and Giordan, D.: Landslide early warning based on failure forecast models: the example of the Mt. de La Saxe rockslide, northern Italy. Nat. Hazards Earth Syst. Sci., 15~~,~~: 1639–1644~~, 2015~~, doi:10.5194/nhess-15-1639-2015, 2015.

Margottini, C., Antidze, N., Corominas, J., Crosta, G.B., Frattini, P., Gigli, G., Giordan, D., Iwasaky, I., Lollino, G., Manconi, A., Marinos, P., Scavia, C., Sonnessa, A., Spizzichino, D., and Vacheishvili, N.: Landslide hazard, monitoring and conservation strategy for the safeguard of Vardzia Byzantine monastery complex, Georgia. Landslides 12:193–204, doi:10.1007/s10346-014-0548-z, 2015.

Marinos, V., Marinos, P., and Hoek, E.: The geological strength index: applications and limitations. Bull Eng Geol Environ 64: 55–65, doi:10.1007/s10064-004-0270-5, 2005.

Martino, S., and Mazzanti, P.: Integrating geomechanical surveys and remote sensing for sea cliff slope stability analysis: the Mt. Pucci case study (Italy). Nat. Hazards Earth Syst. Sci., 14, 831-848, doi:10.5194/nhess-14-831-2014, 2014.

Mateos, R.M., García-Moreno, I., Reichenbach, P., Herrera, G., Sarro, R., Rius, J., Aguiló, R., and Fiorucci, F.: Calibration and validation of rockfall modeling at regional scale: application along a roadway in Mallorca (Spain) and organization of its management. Landslides 13:751–763, doi:10.1007/s10346-015-0602-5, 2016.

Mathworks Matlab mathematical environment (Matlab) available at: https://www.mathworks.com/products/matlab.html, (last access 1 February 2017), 2017

Michoud, C., Derron, M.-H., Horton, P., Jaboyedoff, M., Baillifard, F.-J., Loye, A., Nicolet, P., Pedrazzini, A., and Queyrel, A.: Rockfall hazard and risk assessments along roads at a regional scale: example in Swiss Alps. Nat. Hazards Earth Syst. Sci., 12, 615–629, 2012. doi:10.5194/nhess-12-615-2012, 2012.

Milenkovic, M.,Karel, W., Ressl, C., Pfeifer, N.: A comparison of UAV and TLS data for soil roughness assessment, ISPRS Annals of the Photogrammetry, Remote Sensing and Spatial Information Sciences, Volume III-5, pp. 145-152, doi:10.5194/isprsannals-III-5-145-2016, 2016.

Naumann, M., Geist, M., Bill, R., Niemeyer, F., Grenzdörffer, G.: Accuracy comparison of digital surface models created by unmanned aerial systems imagery and terrestrial laser scanner, International Archives of the Photogrammetry, Remote Sensing and Spatial Information Sciences, Volume XL-1/W2, pp. 281-286, 2013.

Neugirg, F. Stark, M. Kaiser A., Vlacilova M., Della Seta M., Vergari F., Schmidt J.,. Becht M, Haas F. Erosion processes in calanchi in the Upper Orcia Valley, Southern Tuscany, Italy based on multitemporal high-resolution terrestrial LiDAR and UAV surveys. Geomorphology, 269, 8-22. doi: 10.1016/j.geomorph.2016.06.027, 2016.

Nex, F., Rupnik, E., Toschi, I., Remondino, F., Automated processing of high resolution airborne images for earthquake damage assessment. International Archives of Photogrammetry and Remote Sensing and Spatial Information Sciences, 41. 315-321. doi:10.5194/isprsarchives-XL-1-315-20, 2014.

Niethammer, U., James, M.R., Rothmund, S., Travelletti, J., Joswig, M. UAV-based remote sensing of the Super-Sauze landslide: Evaluation and results. Engineering Geology 128, 2-11, doi: 10.1016/j.enggeo.2011.03.012, 2012.

Pappalardo, G., Mineo, S., and Rapisarda, F.: Rockfall hazard assessment along a road on the Peloritani Mountains (northeastern Sicily, Italy) Nat. Hazards Earth Syst. Sci., 14, 2735-2748, doi:10.5194/nhess-14-2735-2014, 2014.

Pix4D photogrammetry software (Pix4D) available at: https://pix4d.com/product/pix4dmapper-pro/ (last access 1 February 2017), 2017

583 Prokop, A.; Panholzer, H.: Assessing the capability of terrestrial laser scanning for monitoring slow moving landslides. Nat.
584 Hazard. Earth Syst. Sci. 9, 1921–1928, https://doi.org/10.5194/nhess-9-1921-2009, 2009.
585 Rau, J., Jhan, J., Lob, C., Linb, Y. Landslide mapping using imagery acquired by a fixed-wing UAV. ISPRS – Int. Arch.
586 Photogramm. Remote Sens. Spatial Inform. Sci. XXXVIII-1/C22, 195–200, 2011.
587 Real time kinematic net service (RTKnet) available at: https://www.gnssnet.hu (last access 1 February 2017), 2013
588 ~~Rothmund, S., Niethammer, U., Walter, M., Joswig, M.: Comparison of DSMs acquired by terrestrial laser scanning, UAV-~~
589 ~~based aerial images and ground based optical images at the Super Sauze landslide, EGU General Assembly Conference~~
590 ~~Abstracts, 2013.~~
591 Remondino, F., Barazzetti, L., Nex, F., Scaioni, M., Sarazzi, D.: UAV Photogrammetry for mapping and 3D modelling –
592 Current status and future perspectives. International Archives of the Photogrammetry, Remote Sensing and Spatial
593 Information Sciences, Volume XXXVIII-1/C22, 2011
594 Remondino, F., Spera, M.G. Nocerino E., Menna F., Nex F.: State of the art in high density image matching. The
595 Photogrammetric Record, 29(146): 144-166, DOI: 10.1111/phor.12063, 2014.
596 Rupnik, E., Nex, F., Toschi, I., Remondino, F.: Aerial multi camera systems: Accuracy and block triangulation issues.
597 ISPRS Journal of Photogrammetry and Remote Sensing, 101, 233-246, https://doi.org/10.1016/j.isprsjprs.2014.12.020,
598 2015.
599 Salvini, R., Mastrorocco, G., Seddaiu, M., Rossi, D., Vanneschi, C.: The use of an unmanned aerial vehicle for fracture
600 mapping within a marble quarry (Carrara, Italy): photogrammetry and discrete fracture network modelling. Geomatics,
601 Natural Hazards and Risk, 8(1), 34-52, doi:10.1080/19475705.2016.1199053, 2017.
602 Samodra, G., Chen, G., Sartohadi, J., Hadmoko, D.S., Kasama, K., and Setiawan, M.A.: Rockfall susceptibility zoning based
603 on back analysis of rockfall deposit inventory in Gunung Kelir, Java. Landslides ~~(2016),~~ 13~~:~~, 805–819,
604 doi:10.1007/s10346-016-0713-7., 2016.
605 Scaioni , M., Longoni, L., Melillo, V. Papini, M.: Remote Sensing for Landslide Investigations: An Overview of Recent
606 Achievements and Perspectives. Remote Sensing, 6 (10), 9600-9652, doi:10.3390/rs6109600, 2014.
607 Stead, D. Wolter A. A critical review of rock slope failure mechanisms: The importance of structural geology. J. Structural
608 Geology, 74, 1-23. doi: 10.1016/j.jsg.2015.02.002, 2015.
609 Stück, H., Forgó, L.Z., Rüdrich, J., Siegesmund, S., Török, Á.: The behaviour of consolidated volcanic tuffs: weathering
610 mechanisms under simulated laboratory conditions, Environmental Geology, Vol. 56(3-4), 699-713, doi:10.1007/s00254-
611 008-1337-6, 2008.
612 Tannant D.D. Review of Photogrammetry-Based Techniques for Characterization and Hazard Assessment of Rock Faces,
613 International Journal of Geohazards and Environment, Vol 1 (2), 76-87, https://doi.org/10.15273/ijge.2015.02.009, 2015.
614 Tannant, D.D., Giordan, D., Morgenroth, J.: Characterization and analysis of a translational rockslide on a stepped-planar
615 slip surface. Engineering Geology, 220, 144-151, https://doi.org/10.1016/j.enggeo.2017.02.004, 2017.
616 Török, Á., Forgó, L.Z. Vogt, T., Löbens, S., Siegesmund, S., and Weiss, T.: The influence of lithology and pore-size
617 distribution on the durability of acid volcanic tuffs, Hungary. Prykril, R. & Smith, J.B. (Eds.): Building Stone Decay:
618 From Diagnosis to Conservation, Geological Society, London, Special Publications 271: 251-260, 2007.
619 Vásárhelyi B.: Influence of the water saturation for the strength of volcanic tuffs. In: Dinis da Gama C., Ribeiro e Sousa L.
620 (eds). Workshop on volcanic rocks.Proccedings, Lisboa, 89-96. 2002
621 Westoby M.J., Brasington J., Glasser N.F., Hambrey M.J., Reynolds J.M. Structure-from-Motion' photogrammetry: A low-
622 cost, effective tool for geoscience applications, Geomorphology, Volume 179, Elsevier, pp. 300–314, doi:
623 10.1016/j.geomorph.2012.08.021, 2012.
624 Z+F terrestrial laser scanner (Z+F) available at: http://www.zf-laser.com/Z-F-IMAGER-R-
625 5010C.3d_laserscanner.0.html?&L=1 (last access 1 February 2017), 2014.